

## HIGH FREQUENCY OF RECOMBINATION-DRIVEN ALLELIC DIVERSITY AND TEMPORAL VARIATION OF *PLASMODIUM FALCIPARUM* *MSP1* IN TANZANIA

KAZUYUKI TANABE,\* NAOKO SAKIHAMA, INGEGERD ROTH, ANDERS BJÖRKMÄN, AND ANNA FÄRNERT

Laboratory of Malariology, International Research Center of Infectious Diseases, Research Institute for Microbial Diseases, Osaka University, Suita, Osaka 565-0871, Japan; Nyamisati Malaria Research Unit, Dar es Salaam, Tanzania; Unit of Infectious Diseases, Department of Medicine, Karolinska Institute, Karolinska University Hospital, Stockholm, Sweden

**Abstract.** A major mechanism for the generation allelic diversity in the *Plasmodium falciparum* *msp1* gene is meiotic recombination in the *Anopheles* mosquito. The frequency of recombination events is dependent on the intensity of transmission. Herein we investigate the frequency of recombination-driven allelic diversity and temporal variation of *msp1* in Rufiji, eastern coastal Tanzania, where malaria transmission is intense. We identified 5' recombinant types, 3' sequence types, and *msp1* haplotypes (unique associations of 5' recombinant types and 3' sequence types) to measure the extent and temporal variation of *msp1* allelic diversity. The results show that *msp1* haplotype diversity is higher in Tanzania as compared with areas with lower transmission rates. The frequencies of individual polymorphic regions/sites remained stable during the study period. However, the frequency distribution of *msp1* haplotypes varied between 1993 and 1998. These results suggest that frequent recombination events between *msp1* alleles intermittently generate novel alleles in high transmission areas.

### INTRODUCTION

The 200-kDa merozoite surface protein-1 (MSP-1) of *Plasmodium falciparum* is a leading vaccine candidate antigen.<sup>1,2</sup> MSP-1 contains at least two regions targeted by host immunity: block 2 near the N terminus and block 17 at the C terminus. Human antibodies against block 2 are associated with protection from clinical malaria in highly endemic areas in Africa.<sup>3</sup> Block 17 encodes a C-terminal 19-kDa polypeptide, a product processed from MSP-1,<sup>4</sup> which confers protection after immunization against challenge with live parasites in animals.<sup>5,6</sup> Sera from individuals living in highly endemic areas contain antibodies against the 19-kDa fragment that inhibit merozoite invasion into red blood cells.<sup>7-9</sup>

MSP-1 exhibits extensive polymorphism,<sup>10,11</sup> which is a potential obstacle to the development of effective vaccines. In animal models, MSP-1 has been shown to be the major antigen involved in inducing "strain-specific immunity," in which the host mounts an immune response that is more effective against the immunizing strain than it is against genetically divergent strains.<sup>12,13</sup> As is the case for other *P. falciparum* antigen genes, *msp1* polymorphism is generated via a number of different mechanisms: point mutations result in single-nucleotide polymorphisms (SNPs), insertion/deletion of repeats cause repeat length polymorphisms, and meiotic recombination involving the exchange of gene fragments between parental alleles produces novel alleles in the progeny. SNPs in *msp1* appear to be stable through time<sup>14</sup> and may be of ancient origin.<sup>15</sup> Repeat-length polymorphisms are common in *msp1*<sup>10,11,16</sup> to the extent that size polymorphism between alleles is widely used as a marker for parasite genotyping.<sup>17</sup> Aside from repeat-length polymorphisms, meiotic recombination is the major mechanism for the generation of *msp1* allelic diversity.<sup>10</sup> Potential recombination sites have previously been mapped to restricted regions within *msp1* (see Figure 1).<sup>10,11</sup> The frequency of recombination in *P. falciparum* is dependent, to a large extent, on the rate of trans-

mission, because meiotic recombination occurs only in the mosquito host. Recombination-driven allelic diversity in *msp1* is expected to be high in areas of intense malaria transmission and lower in areas with less intense transmission dynamics. The validity of this assumption remains to be tested, however, as very few studies have directly measured recombination-driven *msp1* diversity in areas of high transmission.

To investigate the nature and frequency of *msp1* allelic diversity in a highly endemic area, we conducted a study of the prevalence of *msp1* haplotypes in isolates collected 1993, 1998, and 2003 in Rufiji, eastern coastal Tanzania, where malaria transmission is intense and perennial.<sup>18</sup> Our results show that the extent of recombination-driven allelic diversity in *msp1* is higher in Tanzania as compared with areas with lower transmission rates. The frequency distribution of *msp1* haplotypes varied through time, but the frequencies of individual polymorphic regions and sites remained stable throughout the 10-year period of study. These results suggest that frequent recombination events in *msp1* intermittently generate novel *msp1* alleles in a high transmission area.

### MATERIALS AND METHODS

**Study area and sample collection.** *P. falciparum* isolates were collected during malaria surveys from individuals living in Nyamisati village in the Rufiji River Delta, 150 km south of Dar es Salaam, in eastern coastal Tanzania in February and March 1993 ( $N = 120$ ), 1998 ( $N = 132$ ), and January 2003 ( $N = 104$ ). Almost all samples were taken from asymptomatic donors of all ages with a mean age of 14.2 years (range, 1-78) and 16.8 years (range, 1-63) in 1993 and 1998, respectively, and from those aged 10-19 years (mean, 13.8 years) in 2003. Malaria in the study area was holoendemic with perennial transmission with some increase during the two rainy seasons, April to June and December.<sup>18</sup> An annual entomological inoculation rate is not available for the study area, but it is known to be in the range of 94 to 667 in eastern Tanzania.<sup>19</sup> Insecticide-impregnated bed nets were distributed to all houses in the village in 1999. Slide-positive parasite rates were recorded for the 1993 sample (46%) but were unavailable for the other sampling dates because of technical reasons. However, parasite rates as checked by high-sensitivity PCR-based

\* Address correspondence to K. Tanabe, International Research Center of Infectious Diseases, Research Institute for Microbial Diseases, Osaka University, Suita, Osaka, Japan. E-mail: kztanabe@biken.osaka-u.ac.jp

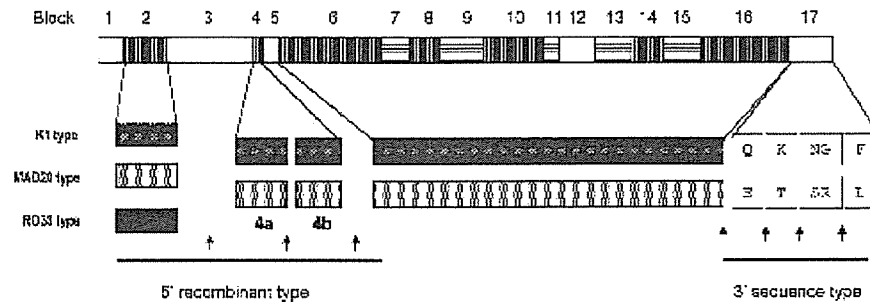


FIGURE 1. Determination of *P. falciparum msp1* haplotype, a unique association of 5' recombinant types and 3' sequence types. *msp1* is divided into 17 blocks, in which inter-allele conserved, semi-conserved, and variable blocks are indicated by open, horizontally hatched, and vertically hatched columns, respectively. For K1-type, MAD20-type, and RO33-type variable blocks, sequences are represented by densely toned, half-toned, and black bars, respectively. The 5' recombinant types were determined by PCR amplification of blocks 2 to 6 using allelic type-specific primers of blocks 2 and 6, followed by nested PCR for blocks 4a and 4b using allelic-specific primers of blocks 4a and 4b. Five amino acid substitutions in block 17 are indicated by the one-letter codes. The 3' sequence type is the combination of those residues. Potential recombination sites are shown by arrows.

parasite detection (*msp1* typing method used in this study) were 78%, 77%, and 44% in 1993, 1998, and 2003, respectively.

All samples were collected after informed consent had been obtained from the donors or their guardians. Venous blood was collected into EDTA-containing tubes and stored at  $-20^{\circ}\text{C}$ . Individuals with signs of clinical disease, i.e., fever and parasites, were treated with Fansidar. Parasite genomic DNA was extracted using the QIAamp DNA Blood Kit (Qiagen, Hilden, Germany). The volume of extracted DNA template was adjusted to be equivalent to the original blood volume. Ethical approval was obtained from the Ethical Committee of the National Institute for Medical Research, Tanzania, and the Ethical Committee of the Karolinska Institute, Sweden. Data previously obtained from clinical samples in Mae Sot in northwestern Thailand in 1995 and from survey samples in Guadalcanal Island in the Solomon Islands in 1994–1996 were used for geographical comparison.<sup>20</sup> We used clinical isolates ( $N = 111$ ) from patients who attended a malaria clinic in Mae Sot in northwestern Thailand in 1995.<sup>21</sup> The mean age of the donors in Thailand was 24.6 years. A total of 90 isolates were collected in north Guadalcanal, the Solomon Islands: 40 clinical isolates from outpatients with a mean age of 18.3 years of a hospital in Honiara City and 50 isolates from four villages (Kaotave, Tadhimboko, Nugalitav, and Ruavatu).<sup>20</sup> In these rural villages, samples were collected in most cases from parasite-positive asymptomatic individuals during malariometric surveys, and most of the donors were primary-school children aged 8 to 15 years.

**Determination of *msp1* polymorphisms.** *P. falciparum msp1* (a 5-kb single-copy gene) consists of 17 distinct sequence blocks, according to the degree of sequence similarity among alleles (Figure 1).<sup>10</sup> Sequence variation in *msp1* is principally dimorphic (either one or the other of two major allelic types: K1 type and MAD20 type) in all variable blocks except block 2, which is trimorphic (represented by K1, MAD20, and RO33 types). To monitor the recombination-driven allelic diversity of *msp1*, we divided the gene into three regions: a 5' 1.1-kb region (blocks 2 to 6), a central 3.5-kb region (blocks 6 to 16), and a 3' 0.4-kb region (block 17), in which potential recombination sites have been mapped to the

5' and 3' regions (Figure 1). No recombination events occur in blocks 6 to 16.<sup>16,21,22</sup> The *msp1* haplotypes are thus defined as unique associations of 5' recombinant types and 3' sequence types in this study.

The 5' recombinant types are defined as unique associations of allelic types of variable blocks 2, 4a, 4b, and 6. In total, 24 distinctive 5' recombinant types are distinguishable: i.e.,  $24 = 3 \times 2 \times 2 \times 2$  (three allelic types designated as K, M, and R in block 2 and two allelic types designated as K and M in blocks 4a, 4b, and 6). The 5' recombinant types were determined by our methods described previously.<sup>20</sup> In brief, they were determined by the following two steps: (i) first-round PCR to determine allelic types of blocks 2 and 6 using allelic-type-specific primers, and (ii) nested PCR to determine allelic types of blocks 4a and 4b ( $\approx 100$  bp) using the first-round PCR products and allelic-type-specific primers. The PCR method allows us to determine the rate of multiple 5' recombinant-type infections, here referred to as "polyinfection rate," and the mean number of 5' recombinant-type infections per isolate (MORT). One microliter of template DNA was used for first-round PCR. 5' Recombinant types were fully determined in 94 of 120 Tanzanian isolates collected in 1993, in 102 of 132 isolates in 1998 samples, and in 46 of 104 isolates in 2003. Thus, 68% (242/356) were PCR-positive in all samples obtained through malariometric surveys, indicating that our data represent a *P. falciparum* population in the study area.

The nucleotide sequence of block 17, which encodes the C-terminal 19-kDa polypeptide, was determined by direct sequencing after amplification of the full-length *msp1*. To see associations of 3' sequence types (block 17 sequences) and 5' recombinant types (blocks 2 to 6), only those isolates having a single 5' recombinant type (i.e., mono-infection) were selected for further analysis. (We did not use cloning of the full-length *msp1* gene because artificial recombination readily occurs during amplification and cloning when samples with mixed genotypes are used.<sup>22</sup>) Because the number of isolates with mono-infections was limited in our Tanzanian samples, we increased the number of mono-infection samples by diluting genomic DNA templates by 20-fold. 5' Recombinant types were again determined for the diluted samples, and those with a single 5' recombinant type were selected. The

numbers of isolates sequenced were 38, 23, and 13 in samples collected in 1993, 1998, and 2003, respectively. No significant difference in the frequency distribution of 5' recombinant types was found between undiluted original samples and diluted samples, indicating no bias of sampling after dilution (not shown). Amplification of the full-length *msp1* was first done with primers UPF1 (5'-GGCTAATGTAAAATGCAAAAATAAATGT) and DWR1 (5'-ACATGACTAAAATATCACTATTCCTGT) in a 20- $\mu$ L reaction mixture containing 1  $\mu$ L of template genomic DNA for 37 cycles using LA-*Taq* (TaKaRa, Tokyo, Japan). Two microliters of 10-fold diluted PCR products were amplified by nested PCR using primers UPF3 (5'-AATAAATGTATACATATTTTGCTAAGTCA) and DWR3 (5'-TTAAGGTAA-CATATTTTAACTCCTACA) for 20 cycles. The PCR product was purified using the QIA Quick PCR purification kit (Qiagen) and directly sequenced from both directions using primers C17aFs (5'-CAAG(G/A)TATGTTAAACA-TTTCACAACA) and DWR3 with the BigDye Terminator Cycle sequencing kit (version 3.1) on an automated multicapillary ABI 3100 sequencer (Applied Biosystems, Foster City, CA). Sequences were verified by re-sequencing the PCR products independently amplified from the same DNA. To date, five major amino acid changes have been identified in block 17 from various geographic areas (E or O at amino acid residue 1644; T or K at 1691; SR or NG at 1700-1701; and L or F at 1716; the positions are numbered according to Ref. 15) (Figure 1).<sup>21,23</sup> Hereafter, we refer to combinations of these residues as 3' sequence type.

Unique associations of 5' recombinant types and 3' sequence types are referred to as *msp1* haplotypes. Partial sequencing of blocks 2 to 6 of the PCR amplicons (full-length *msp1*) confirmed 5' recombinant types determined by PCR-based typing (Tanabe, unpublished). This indicates that our analysis of linkage between polymorphisms in the 5' region and 3' region is not affected by artificial recombination.

**Statistical analyses.** Frequency distributions of *msp1* 5' recombinant types, 3' sequence types, and *msp1* haplotypes were compared using the  $\chi^2$  test with Yates correction and Fisher's exact test for data sets fewer than 5. Differences in mean number of 5' recombinant types per isolate (MORT) were tested for significance using a two-tailed Mann-Whitney *U* test. The diversity level of *msp1* haplotypes was expressed in two ways: (i) relative frequency of the number of unique *msp1* haplotypes per total number of *msp1* haplotypes, and (ii) expected heterozygosity (*h*). *h* and its variance were calculated as previously described.<sup>20</sup> Differences in the relative frequency were tested by *t* test. The frequency of recombination events in *msp1* was inferred from analysis of linkage disequilibrium within and between polymorphic blocks 2 to 6 and polymorphic sites in block 17. To assess linkage disequilibrium within *msp1*, pairs of polymorphic blocks 2, 4a, 4b, and 6 and polymorphic sites in block 17 were subjected to an  $R^2$  test as described elsewhere.<sup>24</sup> Non-informative pairs (frequency < 10% in a polymorphic block or nucleotide site) were excluded from the  $R^2$  test. Significance of linkage disequilibrium was assessed using the  $\chi^2$  test with Yates correction or two-tailed Fisher's exact probability test. A *P* < 0.05 was considered statistically significant.

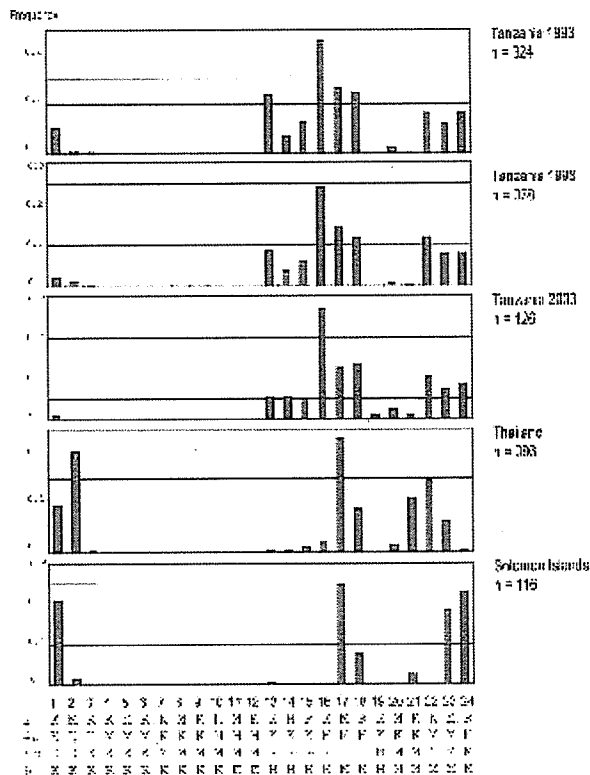


FIGURE 2. Frequency distribution of *P. falciparum msp1* 5' recombinant types in Tanzania. Twenty-four distinct types—unique associations of allelic types in variable blocks 2, 4a, 4b, and 6—are shown at the bottom of the figure. Data from Thailand and Solomon Islands are from Sakihama et al.<sup>20</sup>

RESULTS

***msp1* 5' recombinant types (blocks 2 to 6).** The frequency distributions of *msp1* 5' recombinant types are shown in Figure 2. Types #1 to #12 are those with K1 allelic type in block 6, and types #13 to #24 are those with MAD20 allelic types. Most of the Tanzanian isolates were MAD20 allelic type in block 6 in 1993, 1998, and 2003. The overall pattern of re-

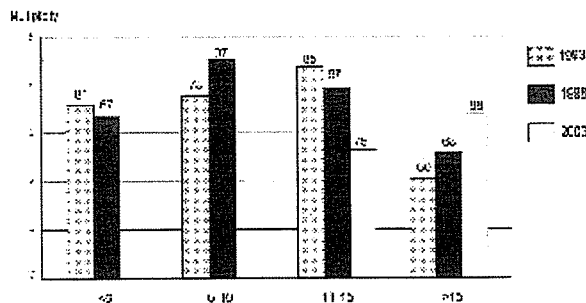


FIGURE 3. Age distribution of mean multiplicity of infection (MORT) in Tanzania. Ages are categorized into four classes: < 6, 6-10, 11-15, and > 15 yrs. MORT is expressed as the number of distinct *msp1* 5' recombinant types per person. Percentage of multiple 5' recombinant infections is shown above each bar.

AU7AUR

quency distribution of 5' recombinant types was very similar from 1993 to 2003. The frequency distribution of 5' recombinant types in Rufiji did not differ significantly from that reported previously in Tanga, northeastern Tanzania.<sup>25</sup> Tanzania was, however, significantly different from other geographic areas: Thailand and Solomon Islands ( $P < 10^{-10}$ ), where frequencies of those types having K1 type in block 6 were substantially higher (19% in Solomon Islands and 30% in Thailand) as compared with Rufiji (< 7%).

Rates of multiple infections of the 5' recombinant types (polyinfection rate) were 76.6%, 87.4%, and 78.3% in 1993, 1998, and 2003, respectively, and the mean number of 5' recombinant types per isolate (MORT) was 3.48, 3.76, and 2.74, respectively. The reduction of MORT from 1998 to 2003 was significant ( $P = 0.008$ , Mann-Whitney  $U$  test). Both polyinfection rate and MORT are considerably higher in Tanzania than in the Solomon Islands (35.4–60.7% for polyinfection rate and 1.41–1.73 for MORT in Solomon Islands<sup>26</sup>). In Thai-

land, the polyinfection rate was 96.3% and MORT was 3.61, a level comparable to that observed in Tanzania. Thai isolates, however, were obtained from symptomatic patients, whereas Tanzanian isolates were from asymptomatic carriers, thus making direct comparison somewhat difficult. (There was no significant difference in polyinfection rate and MORT between individuals with clinical malaria and those with asymptomatic malaria in the Solomon Islands.<sup>20</sup>)

There was a noticeable difference in age distribution of MORT from Tanzania (Figure 3). In 1993, MORT increased from age group < 6 years to age group 11–15 years and thereafter declined. MORT was significantly lower in age group > 15 years than other age groups ( $P = 0.035$  against < 6 years,  $P = 0.001$  against 6–10 years, and  $P = 0.003$  against 11–15 years). In 1998, a peak MORT was observed in age group 6–10 years, followed by a significant reduction in age group > 15 years ( $P = 0.003$ ). In contrast to the reduction in age group > 15 years in 1993 and 1998, MORT increased from age group

TABLE 1  
Frequency distribution of *P. falciparum* *msp1* haplotypes in Tanzania

5' Recombinant type	3' Sequence type					Total	No. of <i>msp1</i> haplotypes
	QKNGL	QKNGF	EKNGL	EKNGF	ETSRL		
Tanzania 1993							
KKKK	1	0	0	0	0	1	
KKKM	2	0	1	0	0	3	
KMKM	2*	3	7	0	1	13	
KMMM	0	1 (QKSGF)	1	0	0	2	
MMKM	0	0	5	0	0	5	
(M/R)MMM	1	0	0	0	0	1	
RKKM	0	0	1	0	0	1	
RMKM	1	3	2*	2	0	8	
RMMM	3	0	0	0	1	4	
Total	10	7	17	2	2	38	20
Tanzania 1998							
MKKK	1	0	0	0	0	1	
KMKM	2	1	8	0	0	11	
KMMM	1 (QTSRL)	1	1	0	0	3	
MKKM	0	0	1	0	0	1	
MMKM	1	1	1	0	1+1 (EKSRL)	5	
RMKM	0	1	0	0	1	2	
Total	5	4	11	0	3	23	15
Tanzania 2003							
KKKK	1	0	0	0	0	1	
KKKM	1	0	0	0	0	1	
KMKM	3	2	2	0	0	7	
MMKM	0	0	0	0	1	1	
RMKM	2*	1	0	0	0	3	
Total	7	3	2	0	1	13	9
Thailand							
KKKK	2	0	0	0	0	2	
MKKK	9	0	4	0	0	13	
KMKM	0	0	0	0	1	1	
MMKM	0	2	12	0	2	16	
RMKM	0	0	3	0	0	3	
RKMM	0	0	3	0	1 (ETSGL)	4	
KMMM	1	1	2	0	3	7	
MMMM	0	0	1	0	1	2	
Total	12	3	25	0	8	48	16
Solomon Islands							
KKKK	9	0	0	0	0	9	
MMKM	1	0	0	0	13	14	
RMKM	0	0	0	0	1	1	
MMMM	0	1	5	0	3	9	
RMMM	0	0	0	0	14	14	
Total	10	1	5	0	31	47	8

Identical *msp1* haplotypes shared between 1993 and 1998 are boxed.  
\* A variant having a substitution from S to N at 1699 is included.

TABLE 2  
Diversity of *P. falciparum msp1* haplotype in Tanzania

	No. of samples	No. of <i>msp1</i> haplotypes	Relative frequency	<i>P</i> value vs. Thailand vs. Solomon	<i>h</i> ± SE*	<i>P</i> value vs. Thailand vs. Solomon
Tanzania						
1993	38	20	0.53	0.040 0.002	0.94 ± 0.02	0.212 0.0002
1998	23	15	0.65	0.007 0.006	0.89 ± 0.06	0.84 0.21
2003	13	9	0.69	0.015 0.002	0.94 ± 0.05	0.515 0.022
Thailand†	52	16	0.31		0.89 ± 0.03	
Solomon Islands	47	8	0.17		0.80 ± 0.03	

\* *h*, expected heterozygosity as an index of haplotype diversity.<sup>26</sup>

† Data from Sakihama et al.<sup>26</sup>

11–15 years to age group > 15 years in 2003, but this trend was not statistically significant. (In 2003, sampling was limited to those of age > 10 years for technical reasons in the survey, and therefore MORT in age groups < 6 years and 6–10 years was not shown.) Polyinfection rates also showed similar patterns of age dependency. A sharp fall was noted from 11–15 years to > 15 years: 85% to 60% in 1993 and 97% to 68% in 1998.

**3' Sequence polymorphism (block 17).** Five major nucleotide polymorphisms in block 17, all resulting in amino acid replacements, were observed in Tanzanian isolates ( $N = 74$ ). We obtained 10 unique 3' sequence types: Q-K-NG-L, Q-T-SR-L, Q-K-NG-F, Q-K-SG-F, E-K-NG-L, E-K-NG-F, E-T-SR-L, and E-K-SR-L (Table 1). In addition, minor variants showing Q-K-NNG-L ( $N = 2$ ) and E-K-NNG-L ( $N = 1$ ) were also observed, where the underlined "N" are substitutions for S at 1699, as detected earlier.<sup>21,23</sup> The number of 3' sequence types was 5 and 4 in Thailand ( $N = 48$ ) and Solomon Islands ( $N = 47$ ), respectively.

**Distribution and diversity of *msp1* haplotypes.** The numbers of distinct *msp1* haplotypes were 20 in 38 isolates in 1993, 15 in 23 isolates in 1998, and 9 in 13 isolates in 2003 (Table 2). The *msp1* haplotype diversity, as expressed by relative frequency of the number of unique *msp1* haplotypes per total number of samples, was high in Tanzania in 1993 to 2003 (0.53–0.69) (Table 2). These levels were significantly higher than the level observed in Thailand (0.31;  $P < 0.04$ ) and Solomon Islands (0.17;  $P < 0.006$ ). Rare *msp1* haplotypes with a frequency of < 5% were abundant in Tanzania as compared with Thailand and Solomon Islands: 21/26 haplotypes (81%) in Tanzania in 1993 and 1998, 10/16 haplotypes (63%) in Thailand, and 3/8 haplotypes (38%) in Solomon Islands. Expected heterozygosity (*h*) was also high from 1993 to 2003 (Table 2). The difference in *h* reached statistical significance in 1993 and 2003 between Tanzania and Solomon Islands but not between Tanzania and Thailand.

**Temporal variation in *msp1* polymorphisms.** The frequencies of polymorphisms in polymorphic blocks 2, 4a, 4b, and 6 and five major polymorphic nucleotide sites in block 17 were compared from 1993 to 2003 (Table 3). A frequency variation was only observed in block 4a. Pairwise comparisons were also made between 1993 and 1998 ( $P = 0.71$ ) and between 1998 and 2003 ( $P = 0.06$ ). In contrast to the stable frequencies of individual polymorphisms, the frequency distribution of *msp1* haplotypes was clearly different between 1993 and 1998 (Figure 4) ( $\chi^2$  test,  $P = 0.001$ ), indicating temporal variation of *msp1* haplotypes during this 5-year interval.

(Rare *msp1* haplotypes were excluded from analysis:  $N = 4$  in 1993 and  $N = 2$  in 1998; see Table 1.) Among 26 distinct haplotypes found in 1993 and 1998 in a total of 61 isolates, only six haplotypes ( $N = 35$ ) were shared between 1993 and 1998. Because of limited numbers of samples, a comparison with samples collected in 2003 was not made. The frequency distribution of *msp1* haplotypes in Tanzania was considerably different from that of Thailand and Solomon Islands ( $\chi^2$  test,  $P < 10^{-10}$ ).

**Linkage disequilibrium in *msp1*.** To determine the frequency of recombination events in *msp1*, we performed linkage disequilibrium (LD) analysis, in which pairs of four polymorphic blocks (blocks 2, 4a, 4b, and 6) and four polymorphic sites were analyzed. Two sites at 1700 and 1701 in block 17 were always linked, and so they were combined for LD analysis. LD was undetectable in most pairs in Tanzania (Figure 5). Only one pair of 10 informative pairs in 1993 ( $N = 37$ ) and one pair of 15 informative pairs in 1998 ( $N = 23$ ) were significant. These pairs were within block 17. LD analysis was not carried out on samples from 2003, due to limited numbers ( $N = 13$ ). These results indicate that the frequency of recombination events in *msp1* is high in the Tanzanian populations. In contrast, in Thailand and Solomon Islands 12 of 21 pairs

TABLE 3  
Stable frequency of polymorphism in *Plasmodium falciparum msp1* in Tanzania

Block	Polymorphic type	<i>n</i> (frequency)			<i>P</i> value
		1993	1998	2003	
2	K1	156 (0.481)	176 (0.466)	56 (0.444)	0.869
	MAD20	79 (0.244)	104 (0.275)	35 (0.278)	
	RO33	89 (0.275)	98 (0.259)	35 (0.278)	
4a	K1	95 (0.293)	84 (0.222)	26 (0.206)	0.048
	MAD20	229 (0.707)	294 (0.778)	100 (0.794)	
4b	K1	247 (0.762)	271 (0.717)	88 (0.698)	0.261
	MAD20	77 (0.238)	107 (0.283)	38 (0.302)	
6	K1	21 (0.065)	13 (0.034)	1 (0.008)	0.06*
	MAD20	303 (0.935)	365 (0.966)	125 (0.992)	
17	1644:Q†	16 (0.432)	9 (0.391)	9 (0.692)	0.339
	1644:E	21 (0.568)	14 (0.609)	4 (0.308)	
	1691:T	2 (0.054)	3 (1.30)	1 (0.077)	
	1691:K	35 (0.946)	20 (0.870)	12 (0.923)	
	1700-01:SR	3 (0.081)	4 (0.174)	1 (0.077)	
	1700-01:NG	34 (0.919)	19 (0.826)	12 (0.923)	
	1716:L	28 (0.757)	19 (0.826)	10 (0.769)	
	1716:F	9 (0.243)	4 (0.174)	3 (0.231)	

\* Comparison between 1993 and 1998. Frequency in 2003 was not informative.

† Positions are after Miller et al.<sup>27</sup>

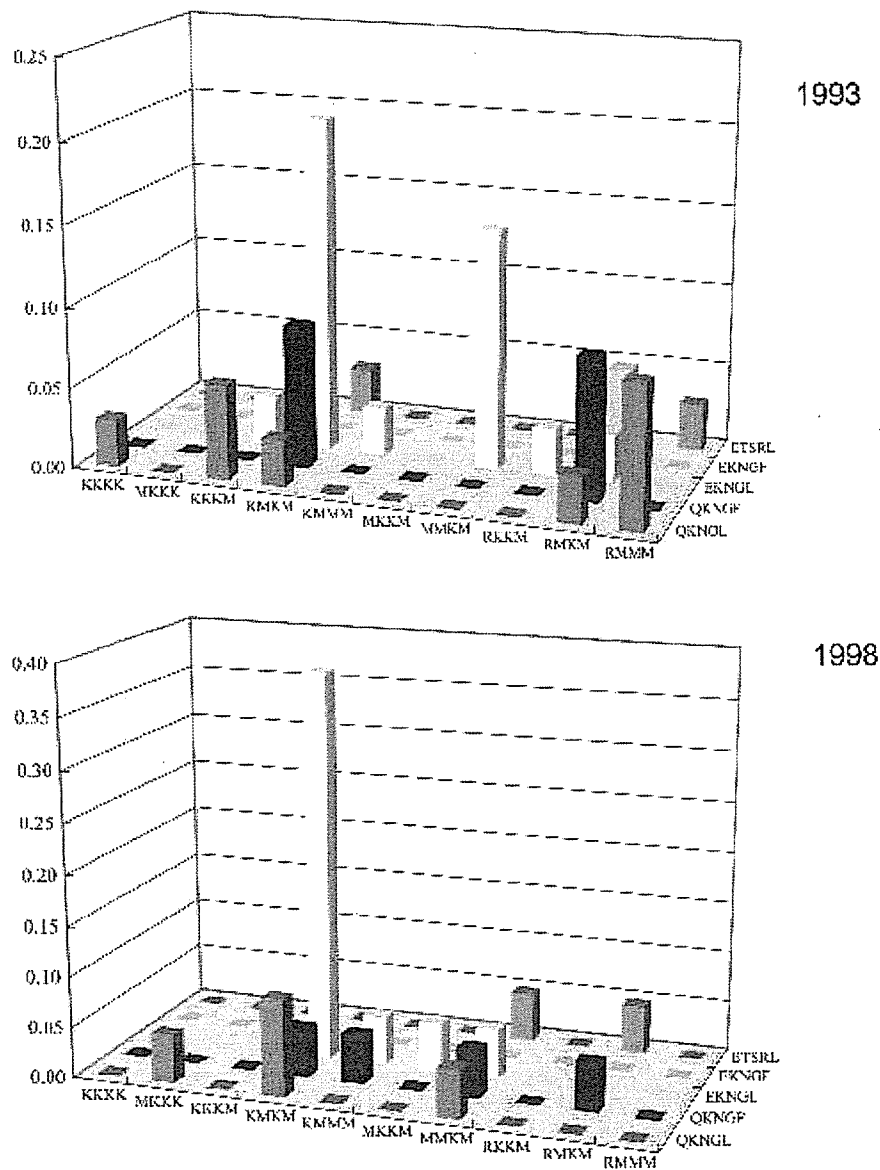


FIGURE 4. Temporal variation in frequency distribution of *P. falciparum msp1* haplotypes between 1993 and 1998. *msp1* haplotypes are unique AU associations of 5' recombinant types (x axis) and 3' sequence types (y axis). Frequencies are shown on the vertical axis.

and 19 of 21 pairs showed LD, indicating limited or little recombination in those areas.<sup>20,24</sup>

#### DISCUSSION

Intragenic meiotic recombination in the mosquito is a major mechanism of generation of allelic variation in *P. falciparum msp1*. The frequency of recombination in *P. falciparum* generally depends on the intensity of malaria transmission, which varies greatly in different endemic areas.<sup>26,27</sup> In areas of Africa experiencing high perennial transmission, the entomological inoculation rate (the number of infective mosquito bites per person per year) can reach several hun-

dred,<sup>19</sup> whereas it is at least 2 orders of magnitude lower in areas of low and seasonal transmission such as Southeast Asia. Thus, the recombination-driven allelic diversity of *msp1* may be assumed to be higher in an intense transmission area than in a low transmission area. The present study is the first to measure the recombination-driven allelic diversity of *P. falciparum msp1* in Africa. The results demonstrate that the diversity of *msp1* haplotypes in Tanzania is high compared with areas of lower transmission such as Southeast Asia and Melanesia.<sup>20</sup> In the present study, geographic comparisons of *msp1* diversity were performed using a PCR-based typing method, which may lead to underestimation of the frequency of recombination events. Nevertheless, we observed a sub-

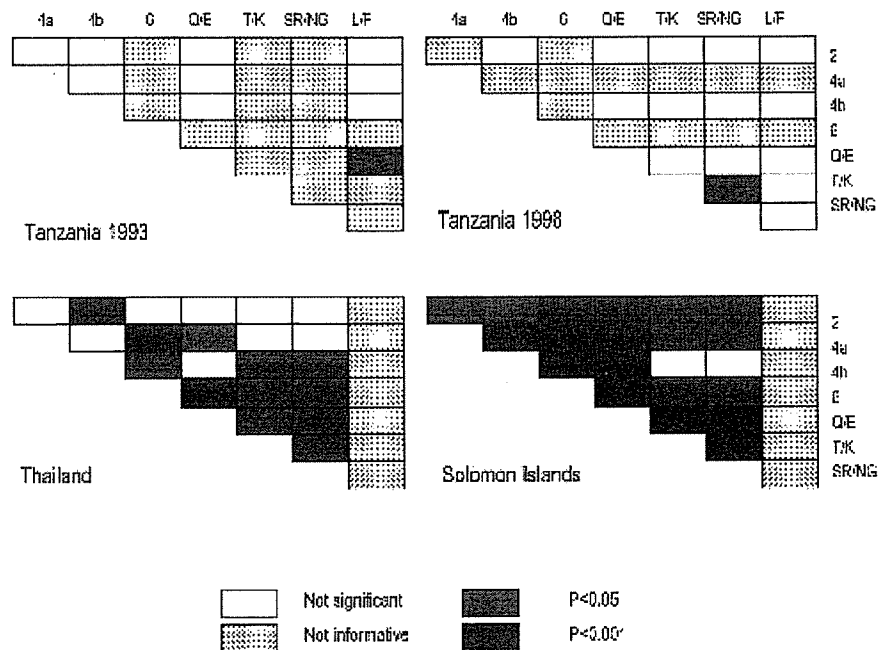


FIGURE 5. Linkage disequilibrium in *P. falciparum* *msp1* in populations from Tanzania. Pairs of polymorphic blocks 2, 4a, 4b, and 6 and four polymorphic sites (Q/E, T/K, SR/NG, and L/F) in block 17 were subjected to the  $R^2$  test. Non-informative pairs (frequency < 10% in a polymorphic block or nucleotide site) were excluded from the  $R^2$  test. Data from Thailand and Solomon Islands are from Sakihama et al.<sup>20</sup>

stantially high frequency of recombination-driven allelic diversity of *msp1*, suggesting that the extent of recombination-driven allelic diversity of *P. falciparum* *msp1* is much higher in Africa than we observed.

Although the intensity of transmission is a major factor determining *msp1* allelic diversity, other factors may also be important. These factors include, but are not necessarily limited to, the rate of multiple-genotype infections (polyinfection rate), the mean number of 5' recombinant type infections per isolate (MORT), and the prevalence of *msp1* haplotypes as well as the parasite-positive rate in a given area. In the Solomon Islands, where the transmission rate is comparable to that of Africa, *msp1* allelic diversity is considerably lower than in Tanzania (Table 3). The polyinfection rate, MORT, and *msp1* haplotype prevalence are relatively limited in the Solomon Islands compared with Tanzania, and therefore the frequencies of out-crossing may be relatively low, resulting in the limited allelic diversity of *msp1* observed in this area.

The frequency distribution of *msp1* haplotypes varied in Nyamisati village between 1993 and 1998. During the same period, frequencies of individual polymorphisms in four polymorphic blocks (blocks 2 to 6) and 4 polymorphic sites (in block 17) remained stable. These two findings appear to contradict each other. However, they are readily reconciled when frequent recombination events are taken into consideration. We observed little linkage disequilibrium in *msp1* in 1993 and 1998, suggesting frequent recombination events in the study area. Therefore, we consider it highly probable that frequent recombination events generate novel *msp1* haplotypes (while simultaneously breaking down previously existing haplotypes), resulting in a temporal variation in their frequency distribution. This explanation is supported by a previous study that showed a rapid decline of linkage disequilibrium

along a map distance in *msp1* in highly endemic areas of Africa.<sup>28</sup> Temporal variations in *msp1* polymorphisms in relatively short periods have been reported in Brazil.<sup>29</sup> Epidemic propagations of parasite populations bearing discrete *msp1* alleles along with human movements have been suggested as a likely reason for such temporal variations. Recombination events may play a minor role, if any, in the temporal variation of *msp1* allelic diversity in low transmission areas.

Variation of the frequency distribution of *msp1* haplotypes through time has important implications regarding the parasite's ability to evade the host's immune response. In highly endemic areas, children gradually gain protective immunity to malaria after repeated infections. Although the mechanisms that generate this protective immunity are little understood, it is believed that protective immunity is acquired by cumulative immune responses to multiple antigenic variants after repeated infections.<sup>30-32</sup> Therefore, the extent and prevalence of antigen diversity in a local area is important for the acquisition of protective immunity. MSP-1 is highly immunogenic and induces antibody responses to the entire MSP-1 molecule.<sup>33</sup> Antibodies specific to different regions of MSP-1 inhibit, when combined, parasite growth in an additive manner.<sup>33</sup> Individuals living in endemic areas raise serum antibodies against MSP-1 in an age-dependent manner.<sup>34</sup> The intermittent appearance of novel *msp1* alleles generated by meiotic recombination would produce a number of novel tertiary structure-associated combinational epitopes, and would therefore be likely to induce "epitope"-specific immunity even when frequencies of individual polymorphic blocks and sites are stable. Human antibodies that inhibit merozoite invasion into red cells are known to recognize conformational epitopes.<sup>9</sup> We consider, therefore, that frequent recombination-driven generation of novel *msp1* alleles may affect the

efficiency of acquiring "strain"-specific immunity in highly endemic areas.

In the context of strain-specific immunity, our observation of a significant reduction of MORT from 1993/1998 to 2003 deserves attention. During this period, the age group displaying the highest MORT shifted from those of ages 6–10 years (highest MORT in 1998) to those > 15 years (highest MORT in 2003). This trend was also seen in the polyinfection rates. The reason for this shift is unknown, but it is possibly related to the introduction of insecticide-treated bed nets (ITNs) to the study village in 1999. ITNs have previously been shown to reduce malaria infections substantially in Tanzania.<sup>35</sup> It is also possible that the establishment of a health clinic with continuous monitoring of malaria infections and provision of early treatment of patients contributed to an overall reduction of the mean number of multiple *mSP2* genotype infections (Bereczky, submitted). The shift of the peak of MORT toward older age groups may be explained in terms of the acquisition of strain-specific immunity. Measures such as ITNs and better health-care facilities will effectively reduce transmission in the areas in which they are deployed. Reduced transmission could lead to an increase in the time it takes an individual to contract, and therefore to develop immunity to, all the different strains present in the area. This would lead to a shift in the peak of MORT to older individuals, as observed in this study. Similarly, the overall reduction of multiple infections may also be a function of reduced transmission.

MSP-1 induces protective antibody responses in individuals living in highly endemic areas.<sup>3,8,9</sup> It may be argued that *mSP1* polymorphism is maintained by immune selection, and hence rare polymorphisms increase in frequency over predominant polymorphisms because of the low rates of acquired immunity against them. However, the present study revealed a very stable frequency distribution of *mSP1* polymorphisms throughout the period of study (10 years) in Tanzania. Polymorphism in *mSP1* has previously been shown to remain stable over a study period of 7 years in the Gambia as determined by typing using monoclonal antibodies.<sup>36</sup> We propose, therefore, that *mSP1* polymorphism is not subject to frequency-dependent immune selection.

In conclusion, the present study demonstrates that allelic diversity of *mSP1* is higher in Tanzania than in Thailand and the Solomon Islands and suggests that intragenic recombination contributes to the allelic diversity of *P. falciparum mSP1* to a greater extent. In Tanzania, frequent recombination events appear to generate novel *mSP1* haplotypes intermittently and cause a temporal variation in the frequency distribution of *mSP1* haplotypes, whereas the frequencies of individual polymorphisms are stable.

Received October 31, 2006. Accepted for publication December 11, 2006.

**Acknowledgments:** The authors thank Richard Culleton for reading this manuscript and his comments. We are grateful to the villagers and the research team in Nyamisati who participated in this study.

**Financial support:** This study was supported by a Grant-in-Aid for Scientific Research on Priority Areas from The Japanese Ministry of Education, Culture, Sports, Science and Technology (18073013), Grants-in-Aid for Scientific Research from the Japan Society for the Promotion of Science (18390131, 18GS03140013), the Japanese Ministry of Health, Labor and Welfare (H17-Sinkou-ippan-019), and the Swedish International Development Agency.

**Authors' addresses:** Kazuyuki Tanabe and Naoko Sakihama, Laboratory of Malariology, International Research Center of Infectious Diseases, Research Institute for Microbial Diseases Osaka University, 3-1, Yamada-Oka, Suita, 565-0871, Japan. Telephone: +81-6-6879-4260, Fax: +81-6-6879-4262, E-mail: kztanabe@biken.osaka-u.ac.jp. Ingegerd Rooth, Nyamisati Malaria Research Unit, P.O. Box, 663, Dar es Salaam, Tanzania. Anders Björkman and Anna Färnert, Unit of Infectious Diseases, Department of Medicine, Karolinska Institute, Karolinska University Hospital, Solna, SE-17176 Stockholm, Sweden.

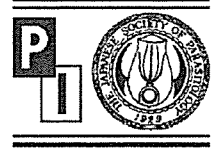
**Reprint requests:** Kazuyuki Tanabe, Laboratory of Malariology, International Research Center of Infectious Diseases, Research Institute for Microbial Diseases Osaka University, 3-1, Yamada-Oka, Suita, 565-0871, Japan. Telephone: +81-6-6879-4260, Fax: +81-6-6879-4262. E-mail: kztanabe@biken.osaka-u.ac.jp.

## REFERENCES

- Holder AA, Guevara Patino JA, Uthaiyibull C, Syed SE, Ling IT, Scott-Finnigan T, Blackman MJ, 1999. Merozoite surface protein 1, immune evasion, and vaccine against asexual blood stage malaria. *Parasitologia* 41: 409–414.
- Mahanty S, Saul A, Miller LH, 2003. Progress in the development of recombinant and synthetic blood-stage malaria vaccines. *J Exp Biol* 206: 3781–3788.
- Conway DJ, Cavanagh DR, Tanabe K, Roper C, Mikes ZS, Sakihama N, Bojang KA, Oduola AMJ, Kremsner PG, Arnot DE, Greenwood BM, McBride JS, 2000. A principal target of human immunity to malaria identified by molecular population genetic and immunological analyses. *Nat Med* 6: 689–692.
- Blackman MJ, Ling IT, Nicholls SC, Holder AA, 1991. Proteolytic processing of the *Plasmodium falciparum* merozoite surface protein-1 produces a membrane-bound fragment containing two epidermal growth factor-like domains. *Mol Biochem Parasitol* 49: 29–34.
- Chang SP, Gibson HL, Lcc-Ng CT, Barr PJ, Hui GS, 1992. A carboxyl-terminal fragment of *Plasmodium falciparum* gp195 expressed by a recombinant baculovirus induces antibodies that completely inhibit parasite growth. *J Immunol* 149: 548–555.
- Kumar S, Yadava A, Keister DB, Tian JH, Ohl M, Perdue-Greenfield KA, Miller LH, Kaslow DC, 1995. Immunogenicity and in vivo efficacy of recombinant *Plasmodium falciparum* merozoite surface protein-1 in *Aotus* monkeys. *Mol Med* 1: 325–333.
- Egan AF, Morris J, Barnish G, Allen S, Greenwood BM, Kaslow DC, Holder AA, Riley EM, 1996. Clinical immunity to *Plasmodium falciparum* malaria is associated with serum antibodies to the 19-kDa C-terminal fragment of the merozoite surface antigen, PfMSP-1. *J Inf Dis* 173: 765–769.
- Nwuba R, Sodeinde O, Anumudu C, Omosu Y, Odaibo A, Holder A, Nwagwu M, 2002. The human immune response to *Plasmodium falciparum* includes both antibodies that inhibit merozoite surface protein 1 secondary processing and blocking antibodies. *Infect Immun* 70: 5328–5331.
- O'Donnell RA, de Koning-Ward TF, Burr RA, Bockarie M, Reeder JC, Cowman A, Crabb B, 2001. Antibodies against merozoite surface protein (MSP)-1<sub>19</sub> are a major component of the invasion-inhibitory response in individuals immune to malaria. *J Exp Med* 193: 1403–1412.
- Tanabe K, Mackay M, Goman M, Scaife JG, 1987. Allelic dimorphism in a surface antigen gene of the malaria parasite *Plasmodium falciparum*. *J Mol Biol* 195: 273–287.
- Miller LH, Roberts T, Shahabuddin M, McCutchan TF, 1993. Analysis of genetic diversity in the *Plasmodium falciparum* merozoite surface protein-1 (MSP1). *Mol Biochem Parasitol* 59: 1–14.
- Martinelli A, Cheesman S, Hunt P, Culleton R, Raza A, Mackinnon M, Carter R, 2005. A genetic approach to the de novo identification of targets of strain specific immunity in malaria parasites. *Proc Natl Acad Sci USA* 102: 814–819.
- Cheesman S, Raza A, Carter R, 2006. Mixed strain infections and strain-specific protective immunity in the rodent malaria parasite *Plasmodium chabaudi chabaudi* in mice. *Infect Immun* 74: 2996–3001.



14. Tanabe K, Sakihama N, Kaneko A, 2004. Stable SNPs in malaria antigen genes in isolated populations. *Science* 303: 493.
15. Polley SD, Weedal GD, Thomas AW, Golightly LM, Conway DJ, 2005. Orthologous gene sequences of merozoite surface protein 1 (MSP1) from *Plasmodium reichenowi* and *P. gallinaceum* confirm an ancient divergence of *P. falciparum* alleles. *Mol Biochem Parasitol* 142: 25–31.
16. Ferreira MU, Ribeiro WL, Tonon AP, Kawamoto F, Rich SM, 2003. Sequence diversity and evolution of the malaria vaccine candidate merozoite surface protein-1 (MSP1) of *Plasmodium falciparum*. *Gene* 304: 65–75.
17. Snounou G, Zhu X, Siripoon N, Jarra W, Thaitong S, Brown KN, Viriyakosol S, 1999. Biased distribution of *mssl* and *mss2* allelic variants in *Plasmodium falciparum* populations in Thailand. *Trans R Soc Trop Med Hyg* 93: 369–374.
18. Rooth I, Björkman A, 1992. Fever episodes in a holoendemic area of Tanzania: parasitological and clinical findings and diagnostic aspects related to malaria. *Trans R Soc Trop Med Hyg* 86: 479–482.
19. Hay SI, Rogers DJ, Toomer JF, Snow RW, 2000. Annual *Plasmodium falciparum* entomological inoculation rates (EIR) across Africa: literature survey, internet access and review. *Trans R Soc Trop Med Hyg* 94: 113–127.
20. Sakihama N, Ohmae H, Bakote B, Kawabata M, Hirayama K, Tanabe K, 2006. Limited allelic diversity of *Plasmodium falciparum mssl* from populations in The Solomon Islands, a highly endemic area. *Am J Trop Med Hyg* 74: 31–40.
21. Sakihama N, Kimura M, Hirayama K, Kanda T, Na-Bangchang K, Jongwutiwes S, Conway D, Tanabe K, 1999. Allelic recombination and linkage disequilibrium within *Mssl* of *Plasmodium falciparum*, the malignant human malaria parasite. *Gene* 230: 47–54.
22. Tanabe K, Sakihama N, Färnert A, Rooth I, Björkman A, Walliker D, Ranford-Cartwright L, 2002. In vitro recombination during PCR of *Plasmodium falciparum* DNA: a potential pitfall in molecular population genetic analysis. *Mol Biochem Parasitol* 122: 211–216.
23. Qari SH, Shi YP, Goldman IF, Nahlen BL, Tibayrenc M, Lal AA, 1998. Predicted and observed alleles of *Plasmodium falciparum* merozoite surface protein-1 (MSP-1), a potential malaria vaccine antigen. *Mol Biochem Parasitol* 92: 241–252.
24. Tanabe K, Sakihama N, Nakamura Y, Kaneko O, Kimura M, Ferreira MU, Hirayama K, 2000. Selection and genetic drift of polymorphisms within the merozoite surface protein-1 gene of *Plasmodium falciparum*. *Gene* 241: 325–331.
25. Ferreira MU, Liu Q, Kimura M, Tanabe K, Kawamoto F, 1998. Allelic diversity in the merozoite surface protein-1 and epidemiology of multiple-clone *Plasmodium falciparum* infections in northern Tanzania. *J Parasitol* 84: 1286–1289.
26. Babiker H, Walliker D, 1997. Current views on the population structure of *Plasmodium falciparum*: implications for control. *Parasitol Today* 13: 262–267. AUS
27. Mu J, Awadalla P, Duan J, McGee KM, Joy DA, McVean GAT, Su AZ, 2005. Recombination hot spots and population structure in *Plasmodium falciparum*. *PLoS Biol* 3: 1734–1741. AUS
28. Conway DJ, Roper C, Oduola AM, Arnot DE, Kremsner PG, Grobusch MP, Curtis CF, Greenwood BM, 1999. High recombination rate in natural populations of *Plasmodium falciparum*. *Proc Natl Acad Sci USA* 96: 4506–4511.
29. Silva NS, Silveira LA, Machado RL, Povoia MM, Ferreira MU, 2000. Temporal and spatial distribution of the variants of merozoite surface protein-1 (MSP-1) in *Plasmodium falciparum* populations in Brazil. *Ann Trop Med Parasitol* 94: 675–688.
30. Beck HP, Felger I, Huber W, Steiger S, Smith T, Weiss N, Alonso P, Tanner M, 1997. Analysis of multiple *Plasmodium falciparum* infections in Tanzanian children during the phase III trials of the malaria vaccine SPf66. *J Inf Dis* 175: 921–926.
31. Contamin H, Fandeur T, Rogier C, Bonnefoy S, Trape JF, Mercereau-Puijalon O, 1996. Different genetic characteristics of *Plasmodium falciparum* isolates collected during successive clinical malaria episodes in Senegalese children. *Am J Trop Med Hyg* 54: 632–643.
32. Färnert A, Rooth I, Svensson A, Snounou G, Björkman A, 1999. Complexity of *Plasmodium falciparum* infections is consistent over time and protects against clinical disease in Tanzanian children. *J Infect Dis* 179: 989–995.
33. Woehlbier U, Epp C, Kauth CW, Lutz R, Long CA, Coulibaly B, Kouyaté B, Arevalo-Herrera M, Herrera S, Bujard H, 2006. Analysis of antibodies directed against merozoite surface protein 1 of the human malaria parasite *Plasmodium falciparum*. *Infect Immun* 74: 1313–1322.
34. Ekaka MT, Jouin H, Lekoulou F, Issifou S, Mercereau-Puijalon O, Ntoumi F, 2002. *Plasmodium falciparum* merozoite surface protein 1 (MSP1) genotyping and humoral responses to allele-specific variants. *Acta Trop* 81: 33–46.
35. Fraser-Hurt N, Felger I, Edoh D, Steiger S, Mashaka M, Masanja H, Smith T, Mbena F, Beck HP, 1999. Effect of insecticide-treated bed nets on haemoglobin values, prevalence and multiplicity of infection with *Plasmodium falciparum* in a randomized controlled trial in Tanzania. *Trans R Soc Trop Med Hyg* 93 (Suppl 1): 47–51.
36. Conway DJ, Greenwood BM, McBride JS, 1992. Longitudinal study of *Plasmodium falciparum* polymorphic antigens in a malaria-endemic population. *Infect Immun* 60: 1122–1127.



## Short communication

The *Plasmodium vivax* homolog of the ookinete adhesive micronemal protein, CTRP<sup>☆</sup>Osamu Kaneko<sup>a</sup>, Thomas J. Templeton<sup>b</sup>, Hideyuki Iriko<sup>c,d</sup>, Mayumi Tachibana<sup>a</sup>, Hitoshi Otsuki<sup>a</sup>, Satoru Takeo<sup>c</sup>, Jetsumon Sattabongkot<sup>e</sup>, Motomi Torii<sup>a</sup>, Takafumi Tsuboi<sup>c,d,\*</sup><sup>a</sup> Department of Molecular Parasitology, Ehime University School of Medicine, Toon, Ehime 791-0295, Japan<sup>b</sup> Department of Microbiology and Immunology, Weill Medical College of Cornell University, New York, NY 10021, USA<sup>c</sup> Cell-Free Science and Technology Research Center, Ehime University, Matsuyama, Ehime 790-8577, Japan<sup>d</sup> Venture Business Laboratory, Ehime University, Matsuyama, Ehime 790-8577, Japan<sup>e</sup> Department of Entomology, Armed Forces Research Institute of Medical Sciences, Phayathai, Bangkok 10400, Thailand

Received 26 January 2006; received in revised form 14 April 2006; accepted 19 April 2006

Available online 5 July 2006

## Abstract

The *Plasmodium* circumsporozoite protein/thrombospondin-related anonymous protein-related protein (CTR<sub>P</sub>) is expressed at the mosquito midgut ookinete stage and is considered to be a transmission-blocking vaccine candidate. CTR<sub>P</sub> is composed of multiple von Willebrand factor A (vWA) and thrombospondin type 1 domains in the extracellular portion of the molecule, and a short acidic cytoplasmic domain that interacts with the actomyosin machinery. As a means to predict functionally relevant domains within CTR<sub>P</sub> we determined the nucleotide sequences of CTR<sub>P</sub> from the *Plasmodium vivax* Sall and the *Plasmodium yoelii* 17XL strains and characterized the conservation of domain architectures and motifs across *Plasmodium* genera. Sequence alignments indicate that the CTR<sub>P</sub> 1st to 4th vWA domains exhibit greater conservation, and thereby are perhaps functionally more important than the 5th and 6th domains. This point should be considered for the development of a transmission-blocking vaccine that includes CTR<sub>P</sub> recombinant subunit. To complement previous cellular studies on CTR<sub>P</sub>, we further determined the expression and cellular localization of CTR<sub>P</sub> protein in *P. vivax* and *P. yoelii*.

© 2006 Elsevier Ireland Ltd. All rights reserved.

**Keywords:** *Plasmodium vivax*; Ookinete; CTR<sub>P</sub>; von Willebrand factor A domain

Malaria parasites possess an apicomplexan-specific class of molecules, termed the TRAP/MIC2 family, which mediate adhesion onto host cell and tissue surfaces, gliding motility, and invasion of host cells. Members of this diverse family of transmembrane proteins are typically composed of one or more von Willebrand factor A (vWA) and thrombospondin type 1 (TSP1) domains in the extracellular portion of the molecule, and

a short acidic cytoplasmic domain that interacts with the actomyosin machinery. Family members include the prototypic thrombospondin-related anonymous protein (TRAP) [1,2] that is expressed in *Plasmodium* sporozoite micronemes; the circumsporozoite protein/thrombospondin-related anonymous protein-related protein (CTR<sub>P</sub>) [3–7], localized to *Plasmodium* ookinete micronemes, and the *Toxoplasma gondii* tachyzoite micronemal protein, TgMIC2 [8]. TRAP/MIC2 family proteins are found across the apicomplexan clade, including NcMIC2 in *Neospora caninum*, Et100 in *Eimeria tenella*, and Em100 in *Eimeria maxima major* [9–11], and predicted homologs within the genome sequence of *Theileria annulata* (TA07755) and *Theileria parva* (TP04\_0306). The *Cryptosporidium parvum* genome sequence lacks extracellular examples of the vWA domain and in this pathogen the predicted TRAP functional homolog (*CpTRAP-C1*) is composed of Apple domains and TSP1 domains [12] (Fig. 1A).

**Abbreviations:** CTR<sub>P</sub>, circumsporozoite protein/thrombospondin-related anonymous protein-related protein; MIDAS, metal ion-dependent adhesion site; TSP1, thrombospondin type 1; vWA, von Willebrand factor A.

<sup>\*</sup> Nucleotide sequence data reported in this paper are available in the GenBank™, EMBL, and DDBJ databases under the accession numbers: AB247368–AB247370.

<sup>\*</sup> Corresponding author. Cell-Free Science and Technology Research Center, Ehime University, Matsuyama, Ehime 790-8577, Japan. Tel.: +81 89 927 8277; fax: +81 89 927 9941.

E-mail address: [tsuboi@ccr.ehime-u.ac.jp](mailto:tsuboi@ccr.ehime-u.ac.jp) (T. Tsuboi).

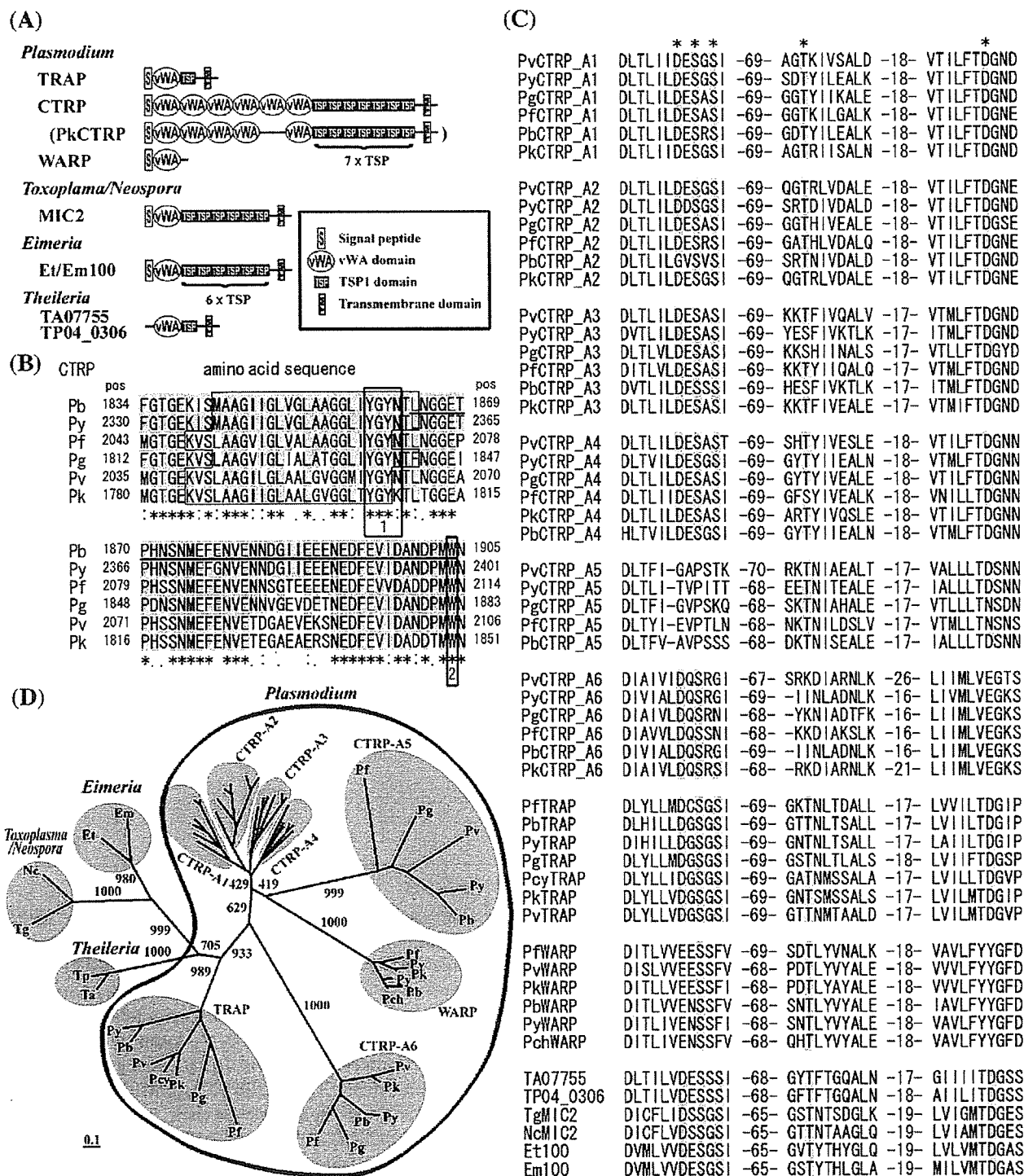


Fig. 1. (A) Schematic diagram of apicomplexan proteins containing vWA and TSP1 domains. Tg, *Toxoplasma gondii*; Et, *Eimeria tenella*; Em, *Eimeria maxima major*; TA, *Theileria annulata*; TP, *Theileria parva*. (B) Amino acid alignment of the transmembrane (boxed with thin line) and cytoplasmic regions of *Plasmodium* CTRP. The underlined region corresponds to that used to generate anti-PbCTRP immune sera recognizing the cytoplasmic tail of PbCTRP (amino acid position 1864–1904). Amino acids identical to those of PbCTRP are shaded. Asterisks indicate the positions where amino acids are identical in all species, and similar amino acids are indicated with colons or periods under the alignments. The tyrosine-based motif involved in cellular trafficking (1) and the tryptophan residue that interacts with the motility actomyosin machinery (2) are boxed with thick lines. (C) Alignment of the MIDAS motif in the apicomplexan vWA domain superfamily. Numbers indicate intervening amino acids separating the three components of MIDAS (DxSxS, T and D, shaded). (D) Phylogenetic analysis of vWA domain of CTRP, TRAP, and WARP. Predicted amino acid sequences were aligned using the MUSCLE multiple sequence alignment program. Phylogenetic trees were constructed with deduced amino acid sequences by using neighbor joining method with Kimura's correction.

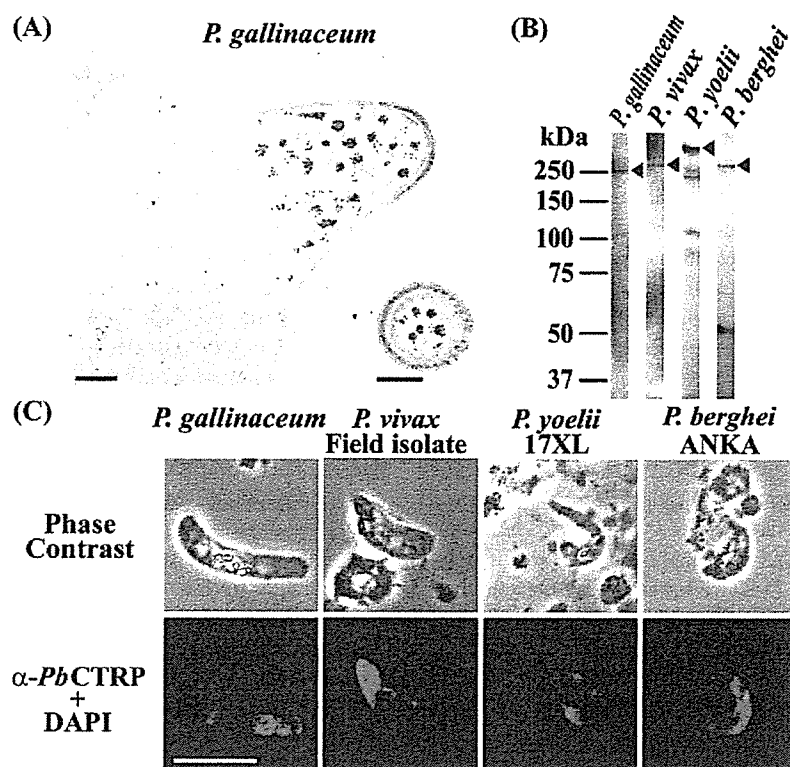


Fig. 2. (A) Immunoelectron microscopy of *P. gallinaceum* ookinetes using rabbit anti-*PbCTRTP* antibody. The immuno-gold particles associated with micronemes and the subpellicular region at the anterior portion. Bars indicate 0.5  $\mu$ m. (B) Western immunoblot analysis of CTRP expression in *P. vivax* and *P. yoelii*. SDS-PAGE was performed with a 7.5% gel under reducing conditions. Proteins were transferred onto a PVDF membrane and reacted with rabbit anti-*PbCTRTP* antibody, followed by horseradish peroxidase-conjugated anti-rabbit IgG, then visualized by chemiluminescence (Immobilon Western Chemiluminescent HRP Substrate; Millipore, Billerica, MA). A band greater than 250 kDa was observed for *P. vivax* and *P. yoelii*. Anonymous bands smaller than 250 kDa were observed for *P. yoelii*, which may represent degraded *PvCTRTP* protein. As a comparison, bands for *PgCTRTP* and *PbCTRTP* were visualized. An anonymous 50-kDa band was detected for *P. berghei*, which was also seen previously [6]. (C) Visualization of *PvCTRTP* and *PyCTRTP* within the ookinete cytoplasm by confocal microscopy. Ookinete-stage parasites of *Plasmodium* parasites were stained with anti-*PbCTRTP* rabbit antibody, followed by FITC-conjugated anti-rabbit IgG. Phase contrast images are shown in the upper panels, and CTRP expression is seen in the cytoplasm of the parasites when FITC images were overlaid with DAPI-stained nuclei (lower panel). Bar indicates 10  $\mu$ m.

The *Plasmodium* ookinete micronemal protein, CTRP, is essential for translocation of mosquito midgut ookinetes to the oocyst stage [4–7], and partial transmission-blocking activity was shown with antibodies recognizing CTRP in *Plasmodium gallinaceum* [13]. CTRP is thereby considered to be a transmission-blocking vaccine candidate. To understand the conservation of CTRP domain architectures and motifs across *Plasmodium* genera, we determined the nucleotide sequences of CTRP from the *Plasmodium vivax* Sall and the *Plasmodium yoelii* 17XL strains, for comparison with previously reported CTRP sequences and those retrieved from the genome sequence databases. To complement cellular studies on CTRP we determined the expression and cellular localization of CTRP protein in *P. vivax* and *P. yoelii*.

A partial DNA sequence of the putative *P. vivax* CTRP (*PvCTRTP*) gene was identified by a TBLASTN search of the *P. vivax* Gene Sequence Tag Project Website [14; accession number, AZ568294] using the amino acid sequence of *PbCTRTP* (AJ238798) as a query. The deduced amino acid sequence of this fragment had homology with the amino acid positions 1295–1464 of *PbCTRTP*, a region that spans the 6th vWA domain and the

first TSP1 domain. Full-length *PvCTRTP* nucleotide sequence was obtained by anchored PCR gene walking as described [15], using four distinct *P. vivax* (Sall) genome DNA splinkerette libraries. PCR-amplified DNA fragments were inserted into the pGEM-T Easy plasmid (Promega, Madison, WI), and nucleotide sequences were determined (AB247369). The gene encoding the *P. yoelii* CTRP (*PyCTRTP*) was isolated from the *P. yoelii* 17XL strain (AB247368), independently from the genome project, using a panel of degenerate oligonucleotides designed based upon alignments of the *pfctrp* (U34363) and *pbctrp* nucleotide sequences. Genomic DNA sequence for the *P. knowlesi* CTRP (*PkCTRTP*) was identified within the contig 4777 at the Sanger Centre website (<http://www.sanger.ac.uk>) following TBLASTN search using *PvCTRTP* amino acid sequence as a query. The reported genomic DNA sequence for the *P. gallinaceum* CTRP (*PgCTRTP*) was incomplete at the carboxy terminus [13; AB247370], and completion of the sequence was achieved using sequence identified within the *P. gallinaceum* genome database at the Sanger Centre website (2570384.c000412673.Contig1).

All CTRP genes possess predicted signal peptide sequences and single transmembrane regions, followed by a short (less than 50

amino acid), acidic cytoplasmic domain at the carboxy terminus (Fig. 1B). Similar to TRAP family members, a tyrosine residue is conserved in all species within the cytoplasmic domain near the transmembrane region; as well as a tryptophan residue at the penultimate amino acid position of the carboxy terminal (Fig. 1B). The tyrosine-based motif is proposed to target trafficking to the micronemes [16]; whereas the tryptophan residue is predicted to be involved in a hydrophobic interaction that is essential for interaction with the subpellicular actomyosin motility network [17]. The overall CTRP domain architecture, composed of six contiguous vWA domains followed by seven contiguous TSP1 domains, is conserved across species boundaries; with the exception that *Pk*CTRP lacks the 5th vWA domain and possesses only five vWA domains (Fig. 1A). Interdomain regions between adjacent vWA domains are easily discernable by characteristic insertions of low complexity proline-rich stretches of charged amino acids. The nucleotide sequence of *Py*CTRP of 17XL strain was identical to that of the 17X nonlethal strain that was used for the *P. yoelii* genome project. *Py*CTRP is notable for a greater than 420 amino acid long insert between the 5th and 6th vWA domains that is composed almost entirely of a repeat of glycine and asparagine residues. This insert is not shared with *Pb*CTRP, despite greater than 86% amino acid similarity throughout the protein.

The vWA domain metal ion-dependent adhesion site (MIDAS) motif [18] is relatively conserved in the first 4 vWA domains of CTRP, but has degenerated in the 5th and 6th vWA domains, and is additionally absent in the *Plasmodium* von Willebrand factor A domain-related protein (WARP) [13,19]. The MIDAS motif consists of a DxSxS consensus at approximately amino acid position 12–16 within each CTRP vWA domain, and threonine and aspartate residues conserved at approximately 89 and 121, respectively (Fig. 1C). This motif is well conserved across apicomplexan parasites and is thus likely to be important for domain function, such as contributing to the correct conformation for the receptor recognition by associating with the divalent metal ion. The MIDAS motif is degenerated in the WARP vWA domain, and because this molecule was found to be a multimer it does not appear that metal binding is essential for the multimerization.

To determine the evolutionary relationships of vWA domains in *Plasmodium* species, the amino acid sequences of this domain were aligned using the MUSCLE algorithm [20] with manual correction (Supplemental figure S1) and a phylogenetic tree was constructed by the neighbor joining method with Kimura's correction with bootstrap value of 1000. As out groups, apicomplexan proteins possessing both vWA and TSP1 domains were included: namely, TgMIC2, NcMIC2, Et100, Emt100, TA07755, and TP04\_0306 (Fig. 1D). The amino acid diversities amongst the CTRP vWA domains are markedly different; for example, the 5th and 6th domains are more divergent compared to the first 4 domains as described [3], but also more diversified among *Plasmodium* species. Thus the functional constraints appear to be relaxed with respect to the 5th and 6th domains in comparison to the 1st through 4th domains, based on the following observations: 1) *Pk*CTRP lacks the 5th vWA domain, 2) the 5th and 6th domains are the most diverse amongst the *Plasmodium* species, and 3) the

MIDAS motif is degenerated in these domains and the ability of receptor recognition is potentially lost. Alternatively, the first 4 vWA domains of CTRP might have evolved by concerted evolution with the gene conversion event between domains before *Plasmodium* speciation. Concerted evolution is known to reduce the diversity between homologous sequences.

The CTRP and WARP vWA domains form a single clade that is distinct from the TRAP vWA domain. This suggests that WARP, which contains a vWA domain but lacks TSP1 domains, originated from a CTRP vWA domain.

Because of the high amino acid sequence similarity (80 to 97.5%) between the cytoplasmic domains of CTRP (Fig. 1B), it was anticipated that cross-species reactivity would be observed for the described purified rabbit antibody to *Pb*CTRP cytoplasmic domain [6]. To evaluate this we performed immunoelectron microscopy using *P. gallinaceum* ookinetes. Indeed, gold particles were found associated with micronemes of mature ookinetes, especially localized at the periphery of each microneme and concentrated in the electron-dense subpellicular region just beneath the apical end (Fig. 2A). The gold particle associated electron-dense region appears to be circumferentially distributed around the apical pole and is consistent with the observed CTRP localization using antibodies specific to *Pg*CTRP [13]. Thus the cross-species reactivity of anti-*Pb*CTRP antibody was verified for *Pg*CTRP. The *Pb*CTRP antibody was further used to detect CTRP orthologs in *P. vivax* and *P. yoelii*. Western immunoblot analyses of ookinetes showed a band with the size slightly greater than 250 kDa for *P. vivax* and excessively greater than 250 kDa for *P. yoelii*. The protein sizes of *Pv*CTRP and *Py*CTRP were greater than those estimated from the amino acid sequences (229 kDa for *Pv*CTRP and 256 kDa for *Py*CTRP, after removing putative signal peptide sequences), which is frequently observed for the malaria proteins. Indeed, control *Pg*CTRP and *Pb*CTRP bands appeared around 250 kDa, which were estimated to be 210 kDa and 213 kDa, respectively (Fig. 2B). By confocal microscopy, anti-*Pb*CTRP antibody demonstrated a cytoplasmic patchy pattern in ookinetes of *P. vivax* and *P. yoelii* with deviated distribution, similar to the pattern for *Pb*CTRP and *Pg*CTRP (Fig. 2C).

In summary, we determined the *Pv*CTRP and *Py*CTRP nucleotide sequences and show protein expression in ookinete stages that is localized to the apical region. Sequence alignments suggest that the CTRP 1st to 4th vWA domains are functionally more important than the 5th and 6th domains. This point should be considered for the development of the recombinant subunits of a transmission-blocking vaccine based on CTRP.

#### Acknowledgements

We thank Dr. M. Yuda for providing anti-*Pb*CTRP rabbit antibody. This work was supported in part by Grants-in-Aid for Scientific Research 16390125 and 16406009 (to T. T.), 15406015 (to M. T.), and 17590372 and 17406009 (to O. K.), and Scientific Research on Priority Areas 16017273 (to T. T.) from the Ministry of Education, Culture, Sports, Science and Technology, Japan. Preliminary sequence data of *P. knowlesi* and *P. gallinaceum* were obtained from the Sanger Institute website at <http://www.sanger.ac.uk/>.

## Appendix A. Supplementary data

Supplementary data associated with this article can be found, in the online version, at doi:10.1016/j.parint.2006.04.003.

## References

- [1] Rogers WO, Malik A, Mellouk S, Nakamura K, Rogers MD, Szarfman A, et al. Characterization of *Plasmodium falciparum* sporozoite surface protein 2. Proc Natl Acad Sci U S A 1992;89:9176–80.
- [2] Sultan AA, Thathy V, Frevert U, Robson KJ, Crisanti A, Nussenzweig V, et al. TRAP is necessary for gliding motility and infectivity of *Plasmodium* sporozoites. Cell 1997;90:511–22.
- [3] Trottein F, Triglia T, Cowman AF. Molecular cloning of a gene from *Plasmodium falciparum* that codes for a protein sharing motifs found in adhesive molecules from mammals and plasmodia. Mol Biochem Parasitol 1995;74:129–41.
- [4] Dessens JT, Beetsma AL, Dimopoulos G, Wengelnik K, Crisanti A, Kafatos FC, et al. CTRP is essential for mosquito infection by malaria ookinetes. EMBO J 1999;18:6221–7.
- [5] Templeton TJ, Kaslow DC, Fidock DA. Developmental arrest of the human malaria parasite *Plasmodium falciparum* within the mosquito midgut via CTRP gene disruption. Mol Microbiol 2000;36:1–9.
- [6] Yuda M, Sawai T, Chinzei Y. Structure and expression of an adhesive protein-like molecule of mosquito invasive-stage malarial parasite. J Exp Med 1999;189:1947–52.
- [7] Yuda M, Sakaida H, Chinzei Y. Targeted disruption of the *Plasmodium berghei* CTRP gene reveals its essential role in malaria infection of the vector mosquito. J Exp Med 1999;190:1711–6.
- [8] Wan KL, Carruthers VB, Sibley LD, Ajioka JW. Molecular characterisation of an expressed sequence tag locus of *Toxoplasma gondii* encoding the micronemal protein MIC2. Mol Biochem Parasitol 1997;84:203–14.
- [9] Tomley FM, Clarke LE, Kawazoe U, Dijkema R, Kok JJ. Sequence of the gene encoding an immunodominant microneme protein of *Eimeria tenella*. Mol Biochem Parasitol 1991;49:277–88.
- [10] Pasamontes L, Hug D, Humbelin M, Weber G. Sequence of a major *Eimeria maxima* antigen homologous to the *Eimeria tenella* microneme protein Etp100. Mol Biochem Parasitol 1993;57:171–4.
- [11] Lovett JL, Howe DK, Sibley LD. Molecular characterization of a thrombospondin-related anonymous protein homologue in *Neospora caninum*. Mol Biochem Parasitol 2000;107:33–43.
- [12] Deng M, Templeton TJ, London NR, Bauer C, Schroeder AA, Abrahamsen MS. *Cryptosporidium parvum* genes containing thrombospondin type 1 domains. Infect Immun 2002;70:6987–95.
- [13] Li F, Templeton TJ, Popov V, Comer JE, Tsuboi T, Torii M, et al. *Plasmodium* ookinete-secreted proteins secreted through a common micronemal pathway are targets of blocking malaria transmission. J Biol Chem 2004;279:26635–44.
- [14] Carlton JM, Dame JB. The *Plasmodium vivax* and *P. berghei* gene sequence tag projects. Parasitol Today 2000;16:409.
- [15] Tsuboi T, Kaslow DC, Gozar MM, Tachibana M, Cao YM, Torii M. Sequence polymorphism in two novel *Plasmodium vivax* ookinete surface proteins, Pvs25 and Pvs28, that are malaria transmission-blocking vaccine candidates. Mol Med 1998;4:772–82.
- [16] Di Cristina M, Spaccapelo R, Soldati D, Bistoni F, Crisanti A. Two conserved amino acid motifs mediate protein targeting to the micronemes of the apicomplexan parasite *Toxoplasma gondii*. Mol Cell Biol 2000;20:7332–41.
- [17] Kappe S, Bruderer T, Gantt S, Fujioka H, Nussenzweig V, Menard R. Conservation of a gliding motility and cell invasion machinery in Apicomplexan parasites. J Cell Biol 1999;147:937–44.
- [18] Lee JO, Rieu P, Arnaout MA, Liddington R. Crystal structure of the A domain from the  $\alpha$  subunit of integrin CR3 (CD11b/CD18). Cell 1995;80:631–8.
- [19] Yuda M, Yano K, Tsuboi T, Torii M, Chinzei Y. von Willebrand Factor A domain-related protein, a novel microneme protein of the malaria ookinete highly conserved throughout *Plasmodium* parasites. Mol Biochem Parasitol 2001;116:65–72.
- [20] Edgar Robert C. MUSCLE: multiple sequence alignment with high accuracy and high throughput. Nucleic Acids Res 2004;32:1792–7.



## Mitochondria and apicoplast of *Plasmodium falciparum*: Behaviour on subcellular fractionation and the implication

Tamaki Kobayashi <sup>a</sup>, Shigeharu Sato <sup>b</sup>, Shinzaburo Takamiya <sup>c</sup>, Kanako Komaki-Yasuda <sup>d</sup>, Kazuhiko Yano <sup>d</sup>, Ayami Hirata <sup>e</sup>, Izumi Onitsuka <sup>e</sup>, Masayuki Hata <sup>a</sup>, Fumika Mi-ichi <sup>a</sup>, Takeshi Tanaka <sup>a</sup>, Toshiharu Hase <sup>f</sup>, Atsushi Miyajima <sup>e</sup>, Shin-ichiro Kawazu <sup>d</sup>, Yoh-ichi Watanabe <sup>a</sup>, Kiyoshi Kita <sup>a,\*</sup>

<sup>a</sup> Department of Biomedical Chemistry, Graduate School of Medicine, The University of Tokyo, 7-3-1 Hongo, Bunkyo-ku, Tokyo 113-0033, Japan

<sup>b</sup> Division of Parasitology, National Institute for Medical Research, The Ridgeway, Mill Hill, London NW7 1AA, UK

<sup>c</sup> Department of Molecular and Cellular Parasitology, Juntendo University School of Medicine, 2-1-1 Hongo, Bunkyo-ku, Tokyo 113-8421, Japan

<sup>d</sup> Research Institute, International Medical Center of Japan, 1-21-1 Toyama, Shinjuku-ku, Tokyo 162-8655, Japan

<sup>e</sup> Laboratory of Cell Growth and Differentiation, Institute of Molecular and Cellular Biosciences, The University of Tokyo, 1-1-1 Yayoi, Bunkyo-ku, Tokyo 113-0032, Japan

<sup>f</sup> Division of Enzymology, Institute for Protein Research, Osaka University, 3-2 Yamadaoka, Suita, Osaka 565-0871, Japan

Received 19 April 2006; accepted 21 September 2006

Available online 9 December 2006

### Abstract

The mitochondrion and the apicoplast of the malaria parasite, *Plasmodium* spp. is microscopically observed in a close proximity to each other. In this study, we tested the suitability of two different separation techniques – Percoll density gradient centrifugation and fluorescence-activated organelle sorting – for improving the purity of mitochondria isolated from the crude organelle preparation of *Plasmodium falciparum*. To our surprise, the apicoplast was inseparable from the plasmodial mitochondrion by each method. This implies these two plasmodial organelles are bound each other. This is the first experimental evidence of a physical binding between the two organelles in *Plasmodium*.

© 2006 Elsevier B.V. and Mitochondria Research Society. All rights reserved.

**Keywords:** *Plasmodium falciparum*; Mitochondrion; Apicoplast; Fluorescence-activated organelle fractionation

### 1. Introduction

Malaria, by far the most important tropical parasitic disease, is caused by a group of parasites *Plasmodium* spp. belonging to the phylum Apicomplexa. Currently, various anti-malarial drug resistant parasite strains are reported and there is a long way for the development of vaccine. Emergence of insecticide resistant mosquito vector limits the current control schemes as well (Greenwood et al.,

2005). In order to control this world problem, studies seeking for unique properties of the parasite are indispensable.

Previous study reported malaria parasites obtain most of their energy from glycolysis, if not all (Roth et al., 1988) and malaria parasite possesses one mitochondrion with various shapes at different stages of the intra-erythrocytic development and it is acristae (Slomianny and Prensier, 1986). Mitochondria of *Plasmodium* species carries 6-kb genome, which is the smallest mitochondrial genome ever been reported and encoding only 3 open reading frames with homology to classical mitochondrial protein, cytochrome *c* oxidase subunit I, cytochrome *c* oxidase subunit III and cytochrome *b*, as well as abbreviated rRNA genes (Vaidya et al., 1989; Feagin, 1992). Thus this

**Abbreviations:** DHOD, dihydroorotate dehydrogenase; FOS, fluorescence-activated organelle sorting; RBC, red blood cell.

\* Corresponding author. Tel.: +81 3 5841 3526; fax: +81 3 5841 3444.

E-mail address: [kitak@m.u-tokyo.ac.jp](mailto:kitak@m.u-tokyo.ac.jp) (K. Kita).

organelle heavily depends on most of the proteins and all tRNAs supplied from the outside.

Biochemical analysis suggested that *Plasmodium falciparum* might lack TCA cycle in the erythrocytic stage (see the review by Sherman, 1979). Recent completion of malaria genome project has revealed that the genes necessary for a complete TCA cycle were present in *P. falciparum* (Gardner et al., 2002). However, it still remains unclear whether the TCA cycle is responsible for the further oxidation of glycolysis product. Nevertheless, the activity of the electron transport chain and the membrane potential of this organelle are indispensable for the survival of the parasite. For example, dihydroorotate dehydrogenase (DHOD) involved in the parasite's *de novo* biosynthesis of pyrimidine requires the functional electron transport chain on the mitochondrial membrane as the electron disposal sink (Gutteridge and Trigg, 1970; Gero et al., 1984; Prapunwatana et al., 1988). More recent study showed that the membrane potential of mitochondria formed by respiration is essential for parasite growth (Srivastava et al., 1999) and complex III (ubiquinol-cytochrome *c* reductase) inhibitor, atovaqone, an anti-malarial that is currently in use is reported to disrupt mitochondrial membrane potential resulting in parasite growth reduction (Srivastava et al., 1997).

Aikawa (1966) carried out an extensive morphological study by electron microscope and found a distinctive organelle in the cell of the malaria parasite. This organelle is multi-membrane bound, always observed adjacent to the mitochondrion (see the review by Bannister et al., 2000). Later, a non-mitochondrial extra-chromosomal DNA encoding a set of genes characteristic of the plastid genome was found in apicomplexan parasites including *Plasmodium* spp. *Toxoplasma gondii* and *Theileria* spp. (Wilson et al., 1996; Kohler et al., 1997) localized the plastid genome-like DNA to the multi-membrane organelle in *T. gondii* by *in situ* hybridization, revealing that the distinctive multi-membrane organelle is the plastid of the apicomplexan parasite. The apicomplexan plastid, which is non-photosynthetic, is often called "the apicoplast" for abbreviation. The genome of the apicoplast is one of the smallest known plastid genomes (Wilson et al., 1996; Gardner et al., 2005). The apicoplast depends heavily on proteins imported post-translationally from the cytosol (see the review by Ralph et al., 2004), as does the mitochondrion.

For biochemical studies of each organelle of *Plasmodium* spp., it is necessary to obtain the pure sample. Fry and Beesley (1991) reported a method to prepare the mitochondria from *Plasmodium* spp. by Percoll density gradient centrifugation. Takashima et al. (2001) reported another preparation method using nitrogen cavitation. The mitochondrial preparation by the latter method exhibited a significantly higher succinate dehydrogenase activity than that by the former method (Takashima et al., 2001). By contrast, no method for preparing the plasmodial apicoplast with a significant purity has been reported.

In this study, we combined nitrogen cavitation method with two different fractionation methods, Percoll density gradient centrifugation or fluorescence-activated organelle sorting (FOS), to prepare the mitochondrion of higher purity from *P. falciparum*. Surprisingly, we found that the mitochondrion and the apicoplast were recovered in the same fraction by each fractionation methods, most likely because the two organelles are bound each other. To our knowledge, this is the first report that suggests the presence of a physical connection between the mitochondrion and the apicoplast of *P. falciparum*.

## 2. Materials and methods

### 2.1. Parasite cultivation and handling

*Plasmodium falciparum* (Honduras-1 strain and 3D7 strain) was cultured following the method reported by Trager and Jensen (1976) with modifications. The culture was maintained with 3% hematocrit type A human red blood cell (RBC) in RPMI 1640 medium (Invitrogen) supplemented with 10% (v/v) type A human serum. Prior to the preparation of crude mitochondrial fraction, parasites were synchronised by 5% (w/v) sorbitol as it was described previously (Lambros and Vanderberg, 1979).

### 2.2. Preparation of the crude *P. falciparum* mitochondria fraction

*Plasmodium falciparum*-infected RBC were collected by centrifugation at 800g for 10 min at 4 °C (LX-120, TOMY) when parasitemia is more than 5% but not exceeding 10%. Parasite was mainly trophozoite stage as it was confirmed by observing the Giemsa's stained smear. Trophozoite stage was considered because DHOD-specific activity is the highest (F. Mi-ichi, Personal communication). The crude *P. falciparum* were disrupted by nitrogen cavitation as described (Takashima et al., 2001). The pellet obtained after the centrifugation at 23,000g for 20 min at 4 °C (Himac CR22, HITACHI) was suspended in 200–400 µl MSE buffer (225 mM mannitol, 75 mM sucrose, 0.1 mM EDTA (Dojin), 3 mM Tris-HCl; pH 7.4) and characterized as a crude mitochondrial fraction (Fig. 1).

### 2.3. Subcellular fractionation of *P. falciparum* mitochondria with the Percoll density gradient centrifugation

The crude mitochondrial fraction prepared from *P. falciparum* Honduras-1 strain (1.5 mg protein) was brought to a total volume of 8 ml in 23% (v/v) Percoll (GE Healthcare) in MSE. Percoll sample was centrifuged at 100,000g for 1 h at 4 °C (Himac SCP70H, HITACHI, rotor No. RP40). Together with the mitochondrial fraction, beads marker provided by the manufacture was centrifuged in parallel to confirm the formation of gradient and density of each fraction. The gradient was fractionated from top to bottom with glass Pasteur pipette (400 µl/ fraction). The formation



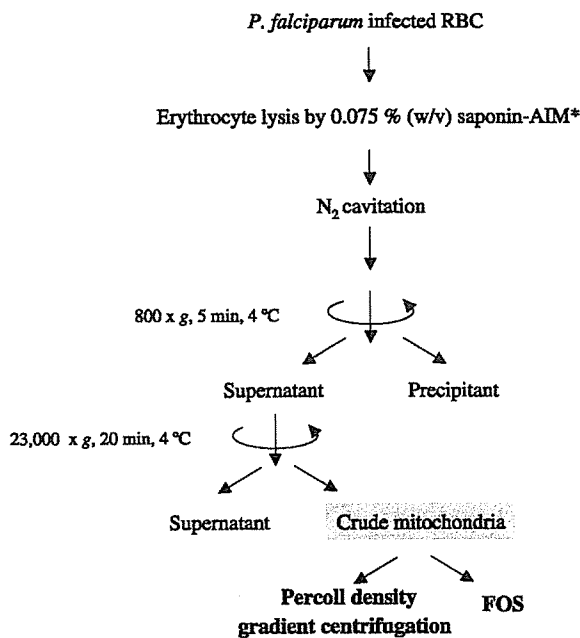


Fig. 1. Crude mitochondria preparation from *P. falciparum* \*AIM (120 mM KCl, 20 mM NaCl, 10 mM Pipes, 1 mM MgCl<sub>2</sub>, 5 mM glucose; pH 6.7).

of the gradient can be affected by factors such as the angle of the rotor. Therefore, it is critical to monitor the formation of the desired gradient by using the density marker beads all the time when one uses different centrifuge and rotor.

DHOD activity was measured to determine the fraction containing mitochondria (Mi-Ichi et al., 2005). DHOD assay was performed at 25 °C using UV3000 spectrophotometer (SHIMADZU) with 1 ml of the reaction mixture containing 45  $\mu$ M 2,6-dichlorophenolindophenol (DCIP) (Sigma), 100  $\mu$ M ubiquinone-2 (Sigma) and 2 mM KCN in 30 mM Tris-HCl (pH 8.0). The reaction was initiated by adding 500  $\mu$ M dihydroorotate and the production of reduced DCIP was monitored at 600 nm ( $\epsilon=21 \text{ mM}^{-1} \text{ cm}^{-1}$ ).

#### 2.4. Protein assay

Protein concentration of *P. falciparum* sample was determined by Bradford method (Bradford, 1976) using Bio-Rad protein assay reagent according to the manual provided by the manufacturer, with bovine serum albumin (PIERCE) as a standard. For the sample that contains Percoll, Percoll was precipitated under the presence of 250 mM NaOH and 0.025% (w/v) Triton X-100 as it was reported (Vincent and Nadeau, 1983) prior to the protein assay.

#### 2.5. Western blot analysis

As Percoll interferes with SDS-PAGE, the fraction of interest was diluted with MSE buffer up to 8.5 ml and

centrifuged at 220,000g for 1 h at 4 °C (CP10 $\alpha$ , 70H, HITACHI) to remove Percoll. Samples were collected as floating pellet and suspended in MSE up to 1.5 ml. Suspended pellet was transferred to 1.5 ml tube and centrifuged at 20,000g for 10 minutes at 4 °C (TOMY MX-160). The pellet was re-suspended in MSE buffer. Prepared samples were then run on 12.5% polyacrylamide gel and transferred to nitrocellulose membrane. Membranes were blocked with 5% (w/v) non-fat skim milk powder in 0.5% (v/v) Tween-Tris-buffered saline and afterwards probed with polyclonal antibodies specific to mitochondrion or apicoplast. For the detection of mitochondrion and apicoplast, serum against recombinant *P. falciparum* iron-sulfur cluster subunit of complex II (rPfIp) and ferredoxin (rPfFd) were raised in mouse and rabbit, respectively. The dilution for the first antibody was 1:2000 for anti-rPfIp serum and 1:1000 for anti-rPfFd serum.

#### 2.6. Electron microscopic observation of the subcellular-fractionated sample by the Percoll density gradient centrifugation

Percoll was removed from the sample as described above. Obtained pellet was suspended in fixative solution containing 2% (v/v) glutaraldehyde in 20 mM sodium phosphate buffer (pH 6.8): MSE buffer = 1:1. The sample was fixed overnight at 4 °C and subsequently washed with 20 mM Sodium phosphate buffer (pH 6.8): MSE buffer = 1:1 for three times. The fixed sample was then dehydrated and embedded in resin. Serial sections were cut and observed by transmission electron microscope (HITACHI H-7100).

#### 2.7. GFP fusion constructs and *P. falciparum* transfection

The expression vector, pSSPF2/PfHSP60-GFP (Sato et al., 2003) was transfected to *Escherichia coli* DH5 $\alpha$  and the transfected *E. coli* was grown in the terrific broth. Plasmids were collected by centrifugation and was purified using Plasmid Maxi Kit (Qiagen). The plasmid was verified with restriction digestion using *Bgl*III and *Xho*I, followed by agarose gel electrophoresis.

The transfection of *P. falciparum* 3D7 was done following the previous report (Sato et al., 2003) with slight modifications. 100  $\mu$ l infected RBC at approximately 10% ring stage parasitemia was suspended in three volumes of cytomix (van den Hoff et al., 1992) containing 50  $\mu$ g of plasmid DNA. Total 400  $\mu$ l of the RBC suspension was electroporated in a 0.2 cm cuvette using Gene Pulser II (Bio-Rad) (0.31 kV, 975  $\mu$ F). After the transfection, parasites were maintained in the medium supplemented with 5 nM WR99210 as it was described previously (Sato et al., 2003).

#### 2.8. Immunofluorescent studies

Infected erythrocytes and mitochondrial fraction was observed using confocal microscope LSM510 (Zeiss).

Parasites expressing fluorescent protein were incubated for 30 min at 37 °C with MitoTracker Red CM-H<sub>2</sub>XRos (Molecular Probes) diluted to 100 nM in culture medium. After the incubation, the culture was once washed with culture medium or AIM medium before microscopy observation.

### 2.9. Flow cytometry analysis and organelle sorting of transfected parasites

*Plasmodium falciparum* 3D7 strain expressing GFP was homogenized by nitrogen cavitation method and the crude mitochondrial fraction was prepared according to the procedure described in the previous section. The prepared mitochondrial fraction was analyzed and sorted by EPICS ALTRA (Beckman Coulter). The size of the sorted particles was determined by Flow Cytometry Size calibration Kit (Molecular Probes). Sorted sample were centrifuged and the precipitant was suspended with MSE.

### 2.10. Detection of organelle by PCR

The primer set to detect apicoplast genome was for the large subunit of rRNA gene, 5'-GAC CTG CAT GAA AGA TG-3' and 5'-GTA TCG CTT TAA TAG GCG-3' as it was described previously (Tan et al., 1997). The primer set to detect mitochondria genome was for the subunit I of Complex IV (cytochrome *c* oxidase), 5'-GAC CCA ACA TTT GCA GGA GAT C-3' and 5'-CAT CAA TGG CAG CAT TAC CTA A-3'. The reaction mixture was prepared with 1 µl of the above mentioned sorted sample (out of final volume 100 µl) or diluted crude mitochondrial fraction, 1× PCR buffer (20 mM Tris-HCl (pH 8.4), 50 mM KCl), 1.25 U *Taq* DNA polymerase (Invitrogen), 1.5 mM MgCl<sub>2</sub>, 200 µM dNTP and 0.25 µM of each primer in a final volume of 50 µl. The volume of samples was determined not to reach the saturation after the PCR cycle.

The PCR was carried out using the following conditions: pre-heating at 95 °C, 3 min; denaturation at 95 °C, 30 s; annealing at 50 °C, 30 s; elongation at 72 °C, 1 min for 30 cycles followed by incubation at 72 °C for 10 min after the final cycle. For the amplification of mitochondrial genome and apicoplast genome, TEMP CONTROL PC-700 (ASTECC) and GeneAmp<sup>®</sup> PCR system 9700 (Perkin-Elmer) was used, respectively. Amplified products were then analyzed on a 1% (w/v) agarose gel.

In the experimental procedure, chemicals used were a special grade and were purchased from Wako unless otherwise stated.

## 3. Results

### 3.1. The mitochondria and apicoplast co-fractionated by the Percoll density gradient centrifugation

Previously, Fry and Beesley (1991) reported a method to prepare plasmodial mitochondria using a density gradient

in 22% (v/v) Percoll formed by centrifugation at 10,000g for 5 min. As this method has been successfully used in other laboratories (Wilson et al., 1992; Krungkrai, 1995; Krungkrai et al., 1997), we preliminarily tested if this method is directly applicable to improve the purity of mitochondria prepared by nitrogen cavitation method, which showed higher enzyme activities of mitochondria than those of previous method (Takashima et al., 2001).

We found method reported by Fry and Beesley (1991) is not sufficient to separate mitochondria as g-force was too low and the time was too short (data not shown). Thus, we examined different conditions of Percoll density gradient centrifugation that might improve the current mitochondria sample. To estimate the purity of the obtained mitochondria, activity of mitochondria-specific enzyme, dihydroorotate dehydrogenase (DHOD), which is localized in the inner membrane of the mitochondria was measured. The increase in DHOD-specific activity indicates the enrichment of mitochondria.

We optimized the condition to be 23% (v/v) Percoll centrifuged at 100,000g for 1 h at 4 °C using Honduras-1 strain. The gradient was confirmed by the control marker beads in each experiment as it is shown in Fig. 2A. After the Percoll density gradient centrifugation of crude mitochondria sample, prominent brown float and dark brown precipitant were observed (Fig. 2A). The density gradient sample was fractionated and recovery profile of the total DHOD activity after the gradient centrifugation showed two peaks (Fig. 2B). The first peak (fractions 8–10) was sharp and more than twice as high total activity as the broad second peak (fractions 12–16). However, owing to the high amount of proteins recovered, the specific activity in the first peak was not improved. By contrast, the second peak of the total activity showed a significantly higher specific activity; the value of fraction 13 ( $66.2 \pm 27.7$  nmol/min/mg protein ( $n = 3$ )) was about 5 times higher than that of the initial sample ( $12.4 \pm 3.01$  nmol/min/mg protein ( $n = 3$ )). Same results were obtained when the fractionations were performed using 3D7 strain.

To assess the degree of contamination of other cell components, the fractions obtained by the Percoll density gradient centrifugation were analysed by electron microscopy. Fractions 13 and 14, which exhibited the highest DHOD-specific activity, contained a number of mitochondria with double membrane (Fig. 3C and D). Interestingly, another type of multi-membrane-bound organelle was also observed adjacent to the mitochondrion (Fig. 3D). A number of hemozoin particles were found in the crude mitochondria preparation before Percoll density gradient centrifugation (Fig. 3A). Fractions 13 and 14 was virtually free from hemozoin particle (Fig. 3B), although other fractions were prevailed by those bodies (Fig. 3E–G). This suggests that the food vacuole was successfully separated from the mitochondrion by the density gradient centrifugation in 23% (v/v) Percoll.

Since the multi-membrane-bound organelle observed adjacent to the mitochondrion seemed to be the apicoplast,

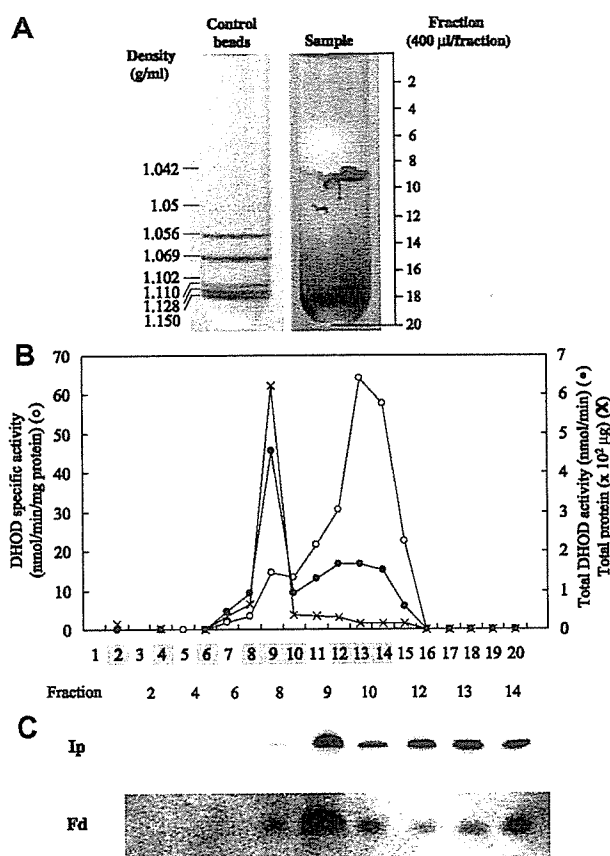


Fig. 2. Percoll density gradient centrifugation. (A) The formation of the gradient was confirmed by beads marker and the density of the control beads were indicated. *P. falciparum* crude mitochondrial fraction was applied to the Percoll density centrifugation forming the brown float and tight brown precipitant. The sample was fractionated from the top to the bottom as indicated. (B) The profile of total protein, DHOD-specific activity and total activity in each fraction of the 23% (v/v) Percoll density gradient centrifugation. The x-axis indicates the fraction number and those highlighted were analyzed by the Western blotting. The approximate location of each fraction is briefly indicated in (A). Total protein (X) DHOD total activity (●) and DHOD-specific activity (○). (C) The Western blot analysis of 23% (v/v) Percoll density centrifugation fractions. The localization of mitochondria and apicoplast were determined by using the specific antibodies. Antibody for mitochondria was for succinate dehydrogenase iron-sulfur cluster subunit (Ip) and antibody for apicoplast was for ferredoxin (Fd). eighty microliters of Percoll density fractionation sample was applied each lane.

we probed the fractions made after 23% (v/v) Percoll density gradient centrifugation with the antibody raised against a protein specifically localizing the mitochondrion or the apicoplast. As shown in Fig. 2C, the distribution profile of ferredoxin (Fd), an apicoplast-localizing protein (Vollmer et al., 2001), overlaps that of the iron-sulfur cluster subunit (Ip) of complex II (succinate-ubiquinone reductase), a mitochondrial integral membrane protein (Takeo et al., 2000). This implies even our improved Percoll density gradient centrifugation is not able to separate the mitochondrion from the apicoplast, although it is enough effective to remove the food vacuole or hemozoin particles.

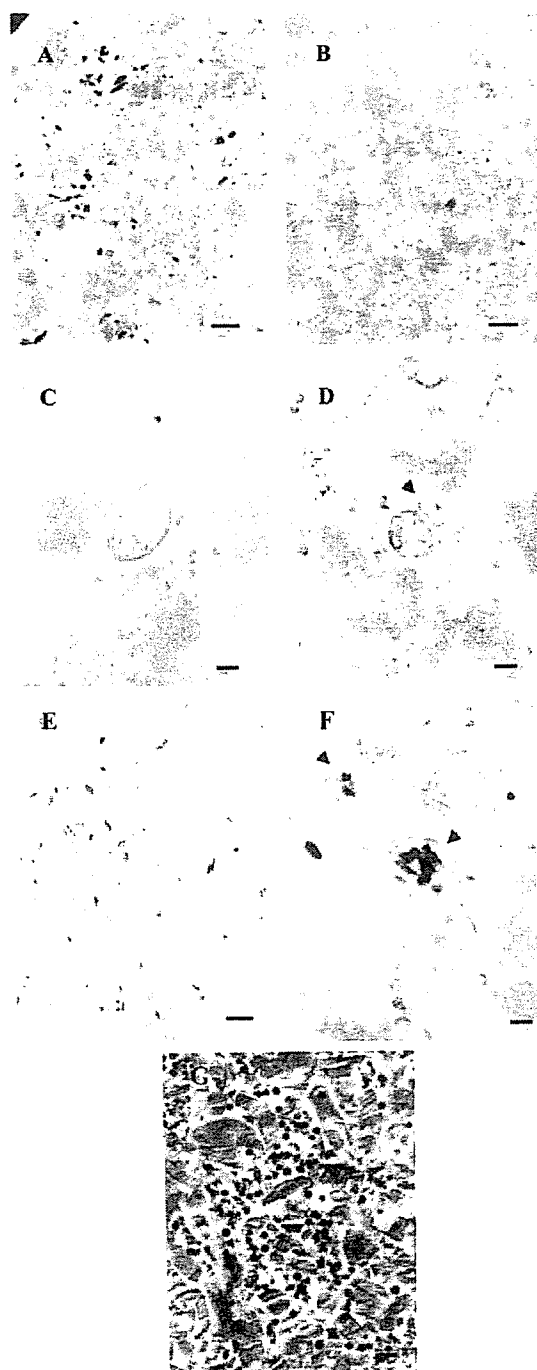


Fig. 3. Electron microscope observation (A) is the crude mitochondria fraction and (B) is the pooled peak fraction of DHOD-specific activity from fraction 13, and 14 after the Percoll density centrifugation (8000 $\times$ ). The dark particles in (A) are significantly reduced in (B), after the Percoll density gradient centrifugation. (C and D) Are observation of the peak DHOD-specific activity at the higher magnification (C; 30,000 $\times$  and D; 15,000 $\times$ ). The double membrane-bound and multi-membrane-bound structures are indicated by arrows. (E and F) Are the observation of the brown float (fraction 9) at 8000 $\times$  and 30,000 $\times$ , respectively. Hemozoin contained in the membrane was observed and from its structure, it is concluded to be a food vacuole. (G) is the tight pellet and the characteristic structure shows it is hemozoin (30,000 $\times$ ). Scale bar; 1  $\mu$ m for 8000 $\times$ , 500 nm for 15,000 $\times$  and 200 nm for 30,000 $\times$  magnification.

### 3.2. The mitochondrion and apicoplast are physically bound to each other; co-fractionation of mitochondrion and apicoplast after the fluorescent-activated organelle sorting

As it was found that Percoll density gradient centrifugation is not suitable to remove the apicoplast from the mitochondrion, next we tested another separation technique based on a different physical property of the organelle to recover the apicoplast-free mitochondria from the crude mitochondrial sample.

*Plasmodium falciparum* 3D7 strain was transfected with a expression plasmid carrying a gene for a GFP derivative that localizes to the mitochondrion (Sato et al., 2003). Specific localization of GFP to the mitochondrion was confirmed by confocal microscope (data not shown) Then, the transfectant and non-transfectant parasites were disrupted by the nitrogen cavitation method and crude mitochondria sample was prepared as it is described in the material and method (Fig. 1). The expression of GFP in mitochondria did not affect the specific activity of mitochondria marker enzyme and therefore the property of mitochondria was not changed at least at the level of electron transfer. In addition, the particle size of the crude mitochondrial sample from GFP-expressing and non-GFP-expressing was not altered depending on the expression of GFP (Fig. 4, inserted figures).

The crude mitochondria fractions prepared from GFP expressing and non-GFP expressing *P. falciparum* was

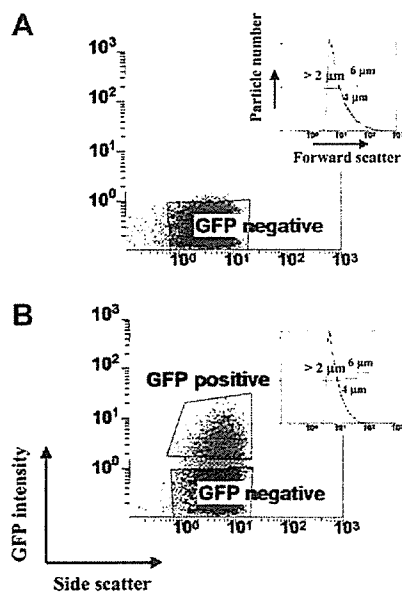


Fig. 4. FOS analysis of crude mitochondria fraction; control and GFP expressing sample. (A) The flow cytometry analysis of the crude mitochondrial fraction from control *P. falciparum* 3D7. The square “GFP negative” indicates the background. (B) The crude mitochondrial fraction prepared from GFP expressing transfectant. The size was determined by the calibration beads. The fraction of the sample expressing significantly high GFP signal were sorted as “GFP positive”. The inserted figures show the particle size of the applied crude mitochondria sample.

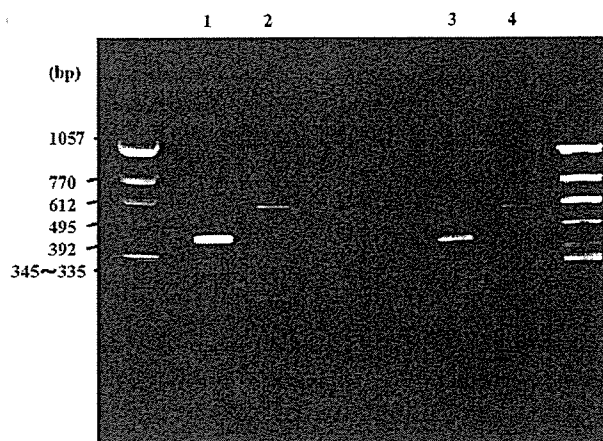


Fig. 5. PCR analysis of mitochondrial fraction and FACS sample. Lanes 1 and 2; crude mitochondria sample. Lane 1 is mitochondria genome-specific primer set and lane 2 is apicoplast genome-specific primer set. Lanes 3 and 4; after the organelle sorting. Lane 3 is mitochondria genome-specific primer set and lane 4 is apicoplast genome-specific primer set. For the detection of mitochondria, the primer set to amplify a part of gene encoding subunit I of cytochrome *c* oxidase was used. For the detection of apicoplast, a part of gene encoding large subunit of ribosomal RNA was used.

analyzed by flow cytometry. The crude mitochondria preparation from the GFP-expressing transfectant emitted significantly higher fluorescence compared to that of non-transfectant control (Fig. 4A and B). We recovered GFP-positive sample after the fluorescence-activated organelle sorting (FOS) and performed PCR to detect the presence of mitochondria using a specific primers for subunit I of cytochrome *c* oxidase, which is encoded on the mitochondrial DNA. Both the crude sample before FOS and the GFP positive fraction recovered after FOS gave a clear band, confirming the presence of the mitochondrial genomic DNA in these samples (Fig. 5, lanes 1 and 3). In addition, PCR product from apicoplast genomic DNA, large subunit of ribosomal RNA, were also detected (Fig. 5, lanes 2 and 4). This result implies that apicoplast were sorted together with mitochondria by FOS.

## 4. Discussion

The biochemical study of plasmodial mitochondria has been limited due to the difficulty to prepare sample with high quality and quantity. Previously we have reported the improved mitochondrial preparation from *P. falciparum* using nitrogen cavitation method (Takashima et al., 2001). In this study, we investigated the method to obtain a mitochondrial preparation of better quality by combining nitrogen cavitation with another fractionation method.

Percoll density gradient centrifugation is a well known method to prepare mitochondrial fraction from various organisms including *P. falciparum* and *Plasmodium yoelii* (Fry and Beesley, 1991). The method also has been used for the subcellular fractionation and purification of